Variations in Velopharyngeal Structure and Function in Adults with Normal and Cleft Anatomy

by

Jillian C. Nyswonger

March, 2015

Director of Thesis: Jamie Perry, PhD

Major Department: Communication Sciences and Disorders

Examination of velopharyngeal (VP) muscle differences among adults with cleft palate is limited. Dynamic assessment of the VP muscles have predominantly been during rest or sustained phonation. The purpose of this study is to examine differences in VP structure and function between adults with repaired cleft palate and adults with normal anatomy at rest and during speech production.

Twelve adult participants (six with normal anatomy, six with repaired cleft palate) completed a 3D static and dynamic MRI protocol. Static image analyses of 12 participants included measures of cranial, velopharyngeal, and levator morphology. Dynamic MRI was obtained in the sagittal and oblique coronal planes during dynamic speech production of "ampa" for 8 participants.

Differences between groups were analyzed using independent sample t-tests ($\alpha < 0.05$). Significant differences between study groups were noted for static measures of posterior cranial base angle, palate length, palate height, pharyngeal depth, and VP ratio. During speech production, significant differences were observed between adults with repaired cleft palate and those with normal anatomy on angular measures of velar height and velar bending during production of selected phonemes within the speech task.

High variability within groups and the limited sample size may have impacted statistical findings. Continued advancements in MRI technology will provide insight into differences in VP function between normal and cleft anatomy and may contribute to a better understanding of the effects of surgical palate repair on physiology for speech production.

Variations in Velopharyngeal Structure and Function in Adults with Normal and Cleft Anatomy

Thesis

Presented To the Faculty of the Department of Communication Sciences and Disorders

East Carolina University

In Partial Fulfillment of the Requirements for the Degree

Master of Science in Communication Sciences and Disorders

by

Jillian Nyswonger

March, 2015

Variations in Velopharyngeal Structure and Function in Adults with Normal and Cleft Anatomy

by

Jillian C. Nyswonger

APPROVED BY:

DIRECTOR OF
THESIS: _____
(Jamie L Perry, PHD)

COMMITTEE MEMBER: _____
(Heather Harris Wright, PHD)

COMMITTEE MEMBER: _____
(Sharilyn Steadman, PHD)

COMMITTEE MEMBER: _____
(Kathleen T. Cox, PHD)

COMMITTEE MEMBER: _____
(Fang Xiangming, PHD)

CHAIR OF THE DEPARTMENT
OF CSDI: _____
(Kathleen T. Cox, PHD)

DEAN OF THE
GRADUATE SCHOOL:_____
Paul J. Gemperline, PhD

TABLE OF CONTENTS

LIST OF TABLES

LIST OF FIGURES

CHAPTER 1: INTRODUCTION

The vocal tract begins above the true vocal folds and includes the nasal, oral, and pharyngeal cavities. In addition to its functions in breathing and swallowing, the vocal tract enables speech production. This region also includes the velopharyngeal (VP) mechanism that functions dynamically during speech production. The VP mechanism is a sphincter-like valve bounded anteriorly by the posterior border of the hard palate and posteriorly by the posterior pharyngeal wall (Skolnick, McCall, & Barnes, 1972). This mechanism includes the posterior pharyngeal wall, lateral pharyngeal walls, and velum. During VP closure, muscles within the VP region function to decouple the oral and nasal cavities during swallowing and production of oral speech sounds (Kuehn, Folkins, & Cutting, 1982; Moon, Smith, Folkins, Lemke, & Gartlan, 1994b).

Several VP muscles impact the sphincter-like action of the mechanism during closure. Coordination of these muscles impacts the degree of velar, lateral pharyngeal wall, and posterior pharyngeal wall movement during VP closure (Moon et al., 1994b). The salpingopharyngeus muscle courses along the lateral pharyngeal walls, but is not thought to significantly impact the function of the VP mechanism. The palatoglossus may play a role in lowering the velum following VP closure and in raising the back of the tongue. The palatopharyngeus consists of vertical and transverse fibers that function to depress the velum during nasal sounds, constrict the pharynx, or raise the larynx. Fibers of the superior pharyngeal constrictor create the superior-lateral and posterior pharyngeal walls and function to achieve closure through a sphincter-like action. The tensor veli palatini muscle functions primarily in opening and closing the Eustachian tube to equalize air pressure and allow for middle ear drainage. The musculus uvulae, also referred to as the uvular muscle, is an intrinsic velar muscle which adds mass to the velum and

makes it easier for the velum to achieve contact with the posterior pharyngeal wall during VP closure.

It is well accepted that the levator muscle is the most important muscle in achieving VP closure (Bell-Berti, 1976; Dickson & Dickson, 1972; Hoopes, Dellon, Fabrikant, & Soliman, 1969a; Moon et al., 1994b). The levator muscle is a paired extrinsic velar muscle that courses anteriorly, inferiorly, and medially from the petrous portion of the temporal bone to insert into the velum (Huang, Lee, & Rajendran, 1998; Kuehn & Moon, 2005). The right and left muscle fibers converge medially and create a sling within the velum (Kuehn & Moon, 2005). Sufficient muscle fibers must exist at the sling in order for it to provide the force necessary to lift the velum up and back towards the posterior pharyngeal wall (Kuehn & Moon, 2005; Liss, 1990). When innervated by the pharyngeal plexus and lesser palatine nerves, the levator muscular sling contracts to elevate and retract the velum (Kuehn & Moon, 2005; Shimokawa, Yi, & Tanaka, 2005).

Cleft Palate Anatomy

In cleft palate anatomy, structures of the vocal tract and articulatory system are altered due to changes in the osseous points of attachment of the associated musculature. Rather than inserting medially in the velum to create a sling, fibers of the levator muscle attach to the lateral and posterior portion of the existing hard palate (Dickson, 1972). Research has demonstrated anatomical differences in those with cleft palate including an altered site of levator attachment, variation in tissue composition within the velum, and muscle hypoplasticity (Dickson, 1972; Fára & Dvorák, 1970; Kuehn & Moon, 2005).

The current understanding of cleft palate anatomy in infants and children is limited because many tools used to evaluate the VP region cannot feasibly be applied to these

populations. Research using MRI has enabled safe visualization of the VP region in these more challenging populations. Perry, Kuehn, Sutton, Goldwasser, and Jerez (2011) observed infants with unrepaired cleft palate to exhibit more acute angles of levator muscle origin at the cranial base compared to those with normal anatomy. Perry et al. (2011) observed more variability in levator muscle length, distance between origin points, velar length, and velar thickness in infants with cleft palate compared to those with normal anatomy. Kuehn, Ettema, Goldwasser, Barkmeier, and Wachtel (2001) diagnosed two 4-year-old children with occult submucous cleft palate through MRI based on visualization of an interruption in the midline tissue of the levator muscle and attachments to the posterior border of the hard palate. Tian et al. (2010a) compared levator muscle morphology in children with repaired cleft palate to children with normal anatomy. Results indicated a slight difference between the two study groups, with children with repaired cleft palate demonstrating shorter levator muscle lengths and more obtuse angles of origin compared to that of children with normal anatomy.

Findings of Ha, Kuehn, Cohen, and Alperin (2007) indicated variable levator muscle length and thickness measurements among four adult males with repaired cleft palate. Measurement of distance between levator muscle origin points, levator muscle length, and thickness were found to be smaller than those observed in adults with normal anatomy by Ettema, Kuehn, Perlman, and Alperin (2002). Ha et al. (2007) suggested increased variability in angles of levator muscle origin and steepness of muscle course was more common in adults with repaired cleft palate than those with normal anatomy. Conclusions, however, may be limited by the relatively small sample size (N=4) and the lack of a within-study comparison control group.

Evaluation of the Velopharyngeal Region

The majority of the current knowledge base surrounding normal and abnormal VP anatomy is based on visualization methods with known limitations. Using histology, Kuehn and Moon (2005) determined that the functional portion of the velum, including the converging of right and left levator bundle fibers at the medial sling, was consistent across normal participants. Mehendale (2004) made efforts to simulate movement of the levator muscle in preserved cadavers and observed traction on the main portion of the levator muscle to result in raising the velum. However, the movement observed likely resulted in much more limited motion than would be expected *in vivo* or fresh living tissue. These methods cannot accurately depict the muscles as they exist in living individuals and may be unreliable due to known changes in tissue composition after death (Dickson & Dickson, 1972; Ettema & Kuehn, 1994; Kuehn & Azzam, 1978; Kuehn & Moon, 2005).

Currently, nasoendoscopy and videofluoroscopy are the most commonly used tools in the clinical evaluation of VP function. However, neither nasoendoscopy nor videofluoroscopy allow visualization of underlying musculature. Pigott (1969) observed the VP region through nasoendoscopy, but no quantitative data could be obtained regarding the morphology of the underlying muscles within the velum. Videos obtained through these methods have been clinically useful, but these videos do not allow for reliable quantitative measurements to be obtained from multiple views or in multiple planes. Skolnick (1970) examined the VP mechanism during speech production based on the assumption that lateral pharyngeal wall movement occurred at the same level of velar movement during closure. Croft, Shprintzen, and Rakoff (1981) examined velopharyngeal closure patterns using nasoendoscopy and videofluoroscopy and noted that closure typically occurred below the level of the posterior nasal spine, contradicting Skonick's (1970) assumption. Nasoendoscopy is invasive, does not provide

consistent views between participants or throughout multiple examinations, and commonly produces a distorted image. Videofluoroscopy exposes patients to radiation, limiting its utility with children and replication. These limitations provide obstacles in the possibility of widespread clinical application because of the need for a non-invasive, risk-free method of visualizing the VP region in living participants during speech production. For additional information regarding the many approaches to imaging of the VP mechanism, see Rowe and D'Antonio (2005), Scott, Wylezinska, Birch, and Miquel (2014), and Witt, Marsh, McFarland, and Riski (2000).

Research using MRI has provided valuable insight suggesting its use as a beneficial tool for the evaluation of the VP region. MRI is the only imaging technique that enables visualization of the musculature of the VP mechanism. MRI and data analysis software enable reliable measurements of the VP structures to be obtained for both normal and abnormal anatomy. Research using MRI has enabled safe, successful visualization of the VP region of typically developing individuals and those with cleft anatomy in infants (Kuehn, Ettema, Goldwasser, & Barkmeier, 2004; Perry et al., 2011), children (Kuehn et al., 2001; Tian et al., 2010a, 2010b, 2010c), and adults (Akgüner et al., 1998; Akgüner, 1999; Bae, Kuehn, Sutton, Conway, & Perry, 2011b; McGowan, Hatabu, Yousem, Randall, & Kressel, 1992; Perry, Kuehn, & Sutton, 2013). However, MRI is limited in its use as a clinical tool due its high cost and limited availability. A challenge in the application of MRI in the evaluation of speech production has been the inability to obtain dynamic images of the VP region during speech. Bae, Kuehn, Conway, and Sutton (2011a) and Sutton et al. (2009) used a head-only MRI scanner to obtain images of the VP region during speech. These scanners produce increased noise in the signal, which negatively impacts image quality. Related to the trade-off between spatial and temporal quality, the use of MRI may also be limited due to the relationship between the strength

of the signal and the amount of noise. The length of time necessary to obtain high-quality images further limits the application and use of MRI with certain populations.

Recent technological advances in MRI protocol enable shorter scan times, optimal image resolution, and reduced motion artifact. These improvements may prove MRI to be a viable option in pre-surgical evaluation and selection of repair technique in cleft palate repair surgeries. The implementation of three-dimensional MRI sequences allows for improved visualization of the underlying musculature within the VP region. Three-dimensional MRI may contribute to recent efforts to apply computer model reconstruction of the VP mechanism clinically (Perry & Kuehn, 2007, 2009). Tian and Redett (2009) observed three-dimensional MRI sequences to be more reliable in selecting the accurate plane of view and in quantitative soft tissue measurements than two-dimensional sequences. Neither Bae et al. (2011a) or Sutton et al. (2009) were able to visualize the full length of the levator muscular sling as it exists in the oblique coronal plane through two-dimensional MRI. Three-dimensional MRI sequences may enable more reliable determination of the oblique coronal plane of view of the levator muscle, a limitation of two-dimensional sequences noted in recent studies (Bae et al., 2011b; Sutton et al., 2009).

MRI presents challenges in its ability to achieve high speed visualizations of articulators during speech production. Gated imaging techniques provide an average view of many repetitions of muscle contractions, such as cyclic contractions of the heart. Kane, Butman, Mullick, Skopec, and Choyke (2002) utilized gated imaging techniques to examine VP functioning during speech. However, muscle contractions during speech production differ from cyclic contractions of the heart because speech production is voluntary and influenced by context. Moon et al. (1994b) observed variability in VP motion across each participant's speech production. Gated imaging techniques may be unreliable in the evaluation of speech production

because speech is not consistent; each person can produce one syllable many different ways without realizing it.

Most MRI studies to date have assessed the VP region while the patient was at rest or during sustained phonation (Atik et al., 2008; Ettema et al., 2002; Ha et al., 2007; Tian & Redett, 2009; Tian et al., 2010a, 2010b, 2010c). Ettema et al. (2002) used static MRI methods to examine levator muscle morphology at rest and during prolonged speech sound production in ten adults with normal anatomy. Ha et al. (2007) conducted a similar study examining four men with repaired cleft palate. Results of these studies indicated adults with repaired cleft palate demonstrated shorter distances between levator muscle origin points, shorter levator muscle lengths, and reduced levator muscle thickness findings than adults with normal anatomy. Ettema et al. (2002) and Ha et al. (2007) documented that levator muscle angle of origin and length values were largest at rest and decreased for production of nasal consonants, low vowels, high vowels, and fricative consonants in adults with normal anatomy and those with repaired cleft palate. The procedures in both studies required participants to sustain speech sounds within the sample for 4 seconds per sound. Sustained phonation tasks do not enable visualization of the rapid and dynamic nature of VP movements that occur during conversational speech production. Rapid dynamic MRI sequences can overcome this limitation and allow visualization of movements as they occur.

Connected speech production is considerably different than sustained phonation of phonemes due to effects of coarticulation and assimilation (Bell-Berti & Krakow, 1990; Bzoch, 1968; Graber, Bzoch, & Aoba, 1959; Moll, 1962). During connected speech, the VP mechanism rapidly alters between fully opened and fully closed in approximately 100 to 150 milliseconds (Kuehn, 1976). By obtaining dynamic MRI images and movies with synchronized audio of

connected speech production, observations may be more clinically applicable. Previous researchers have investigated the application of dynamic MRI techniques in the evaluation of speech and swallowing (Bae et al., 2011a; Maturo et al., 2012; Shinagawa et al., 2005; Sutton et al., 2009; Sutton, Conway, Bae, Seethamraju, & Kuehn, 2010). Recent technological advancements provide the necessary stepping-stones for new protocols in MRI that enable quality audio synchronization with dynamic movies of the vocal tract during speech production (NessAiver, Stone, Parthasarathy, Kahana, & Paritsky, 2006; Sutton et al., 2009; Sutton et al., 2010). Sutton et al. (2009) proposed the benefits of a modified MRI protocol that would allow visualization of the VP region during movements involved in connected speech production. Further investigation by Sutton et al. (2010) led to faster imaging protocols for dynamic image acquisition with adequate field of view and resolution for clear visualization of the vocal tract during speech production. These improvements enabled visualization of the rapid and dynamic soft tissue movements involved in VP closure during speech production in subsequent studies (Bae et al., 2011a; Drissi et al., 2011; Perry, Sutton, Kuehn, & Gamage, 2014).

The present study will address limitations of previously mentioned studies through an improved dynamic MRI protocol and a larger sample size including adults with normal anatomy and adults with repaired cleft palate. This within-study comparison of adults with normal anatomy to adults with repaired cleft palate will overcome limitations in previous studies that only examined one population (Ettema et al., 2002; Ha et al., 2007). The use of an improved dynamic MRI protocol will enable rapid dynamic visualization of muscular movements during each participant's speech production. This study provides an initial examination of velar and levator muscle structure and function in participants with normal and abnormal anatomy at rest and during speech production through quantitative measurements and qualitative analyses.

Quantitative and qualitative differences in velopharyngeal structure and function between the two groups of participants are discussed in detail. The purpose of this study is to examine differences in velopharyngeal structure and function between adults with repaired cleft palate and adults with normal anatomy at rest and during speech production. The following hypotheses were examined:

1) Adults with repaired cleft palate display significant differences in levator muscle and VP structures compared to adults with normal anatomy. In agreement with prior research (Akgüner et al., 1998; Ha et al., 2007; Özgür, Tunçbilek, & Cila, 2000; Satoh, Wada, Tachimura, & Shiba, 2002; Wada, Satoh, Tachimura, & Tatsuta, 1997), it was expected that adult participants with repaired cleft palate would exhibit increased variability in levator and VP morphology, shorter levator muscle length, shorter velar length, and shorter hard palate length indicating a smaller VP ratio than adult participants with normal anatomy.

2) Adults with repaired cleft palate display differences in VP function compared to adults with normal anatomy. In agreement with prior research (Ha et al., 2007; McGowan et al., 2002; Özgür et al., 2000; Satoh et al., 2002; Shinagawa et al., 2005), it was anticipated that adult participants with repaired cleft palate would display differences in VP function including reduced range of velar motion and less levator muscle contractility during speech than adult participants with normal anatomy.

CHAPTER 2: METHOD

Participants

In accordance with the local Institutional Review Boards, 12 English-speaking adults were recruited to participate in this study. Six participants had a history of repaired cleft palate, while six were adults with normal anatomy. Each group included six total participants (three females, three males), for a total of 12 participants with 3D MRI datasets to be analyzed and measured. The average age in the normal anatomy group was 24.79 years (SD: 4.45; Range 20.0-32.33), and the average age of adults with repaired cleft palate was 25.83 years (SD: 6.98; Range 19.5-36.25). Differences in mean age between the two study groups were not significant (p = .18). Average weight for participants with normal anatomy was 66.15 kg (SD: 10.42) and 86.33 kg (SD: 29.5) for those with repaired cleft palate, indicating a significant difference between groups (p = .05). Adults with normal anatomy demonstrated an average height of 172.22 cm (SD: 8.29), which was similar to the average height of 173.57 cm (SD: 9.04) observed in adults with repaired cleft palate (p = .74). The difference in mean group Body Mass Index (BMI) was significant (p = .05), as adults with repaired cleft exhibited a greater mean BMI (28.48 +/- 8.5) than those with normal anatomy (22.25 +/- 2.48). Implications of differences in BMI between adults with repaired cleft palate and those with normal anatomy will be discussed with limitations of this investigation. Participant demographics are displayed in Tables 1 and 2.

Dynamic data are presented for eight out of the 12 total participants, four adults with repaired cleft palate (three females, one male) and four adults with normal anatomy (three females, one male). Due to excessive head motion during acquisition of dynamic MRI data, data from two adults with repaired cleft palate were unusable. Given the focus of the present study on comparing adults with repaired cleft to normal anatomy, two adults with normal anatomy were

also excluded. The two participants with normal anatomy who were excluded from the dynamic portion were selected based on similarities in gender, age, height, and weight to the two adults with repaired cleft palate whose datasets were unusable because of excessive head motion. Excluding these four participants reduced demographic differences in mean age, weight, height, and BMI between the two study groups, as none of these differences were significant for participants included in the dynamic component of this investigation ($\alpha < 0.05$). Eight total participants were successfully scanned using the dynamic MRI protocol.

Magnetic Resonance Imaging

A Siemens 3 Tesla Trio (Erlangen, Germany) MRI scanner and a 12-channel Siemens Trio head coil was used to scan participants in the supine body position, as described in previous literature (Perry et al., 2013; Sutton et al., 2010). All participants were scanned at rest and during real-time speech production. As motion artifact and head movement severely influence MR image quality, an elastic strap attached to the head coil stabilized the head throughout the scan. Participants wore an MR-compatible headset with an attached optical microphone (Dual Channel-FOMR-II, Optocacoustics Ltd., Or Yehuda, Israel) to prevent artifact and background noise from impacting the images. Speech recordings were obtained in real-time following procedures used effectively in previous literature (Bae et al., 2011a; Perry et al., 2014; Sutton et al., 2010). The imaging protocol employed in the present study was developed for research purposes and is not standard to clinical MRI scanners. This advancement in MRI protocol uses a non-Cartesian spiral sequence supported by the 3 Tesla Siemens Trio MRI scanner.

The imaging protocol employed for the dynamic component requires custom pulse sequence programming. A fast-gradient echo FLASH (Fast Low Angle Shot) multi-shot spiral technique was employed to attain the MR images during real-time, dynamic speech production.

This technique allowed acquisition of 15.8 frames per second (fps) and has been described in previous literature as a successful method for use in dynamic MRI assessments of speech (Perry et al., 2014; Sutton et al., 2010). To allow for dynamic estimation and correction of the magnetic field map, a six-shot spiral pulse sequence with an alternating TE between 1.3 and 1.8 ms was employed to acquire high quality images as part of the dynamic MRI protocol (Perry et al., 2014; Sutton et al., 2010). Responses from regions outside the focus area and regions consisting of higher fat content could interfere with visualization of the structures of interest. Multiple saturation bands were employed to reduce signals from these areas to preserve image quality. Parameters of the three-dimensional static and dynamic MRI protocols are provided in Table 3.

Participants were instructed to breathe through their nose throughout the dynamic scanning period. Participants repeated the sequence "ampa" while images are obtained in the sagittal and oblique coronal image planes. The oblique coronal plane was established as the plane along the length of the full levator muscle. The imaging speed enabled visualization of at least one complete image during each lowered and elevated production for data analyses of nasal and oral sounds. Participants heard a metronome through the headphones (rate of 2 Hz) to maintain pace of one syllable per beat. An output time-driven sliding window process reconstructed the images at a desired frame rate of 30 fps. This acquisition rate provided the required data for reconstruction of a single image based on data closest to the desired point in time. This protocol resulted in a minimal level of interpolation over time. It was possible for interpolation of the original frame rate of 15.8 fps to the desired output rate, but it would have caused temporal blurring of data. A benefit to the sliding window reconstruction protocol is that it minimizes repeated temporal information and reduces associated blurring (Sutton et al., 2009). Speech recordings were aligned to dynamic images through acquisition simulation software from

the vendor of the MRI scanner. This acquisition simulation software enabled accurate simulations of sequence timing and provides specific information about the timing of data within 10 ms.

Speech Tasks

To enable dynamic analyses during real-time speech production, participants were instructed to naturally produce one speech task: "ampa." The speech task, "ampa," was used because it is comprised of one nasal syllable, "am," which is produced with the VP port open, and one oral syllable ("pa"), which is produced with the VP port closed. Theoretically, the velum maintains a lowered position during the nasal production and elevates during oral production. Visualization of dynamic MRI videos enabled investigators to visualize transitions between fully lowered and fully elevated velar positions. The "mp" sequence is beneficial because the dynamic change from the VP port open for "m" to closed position for "p" requires rapid movements of the VP mechanism.

Prior to the dynamic component, participants practiced producing the speech task repeatedly to ensure production of the target phoneme throughout. During speech production, participants were in the supine position and instructed to repeat the speech sequence approximately 15 times. Investigators ensured that all data were visualized appropriately.

Image Analyses

Data visualization and analyses occurred in the Cleft Palate Speech Imaging and Visualization Laboratory at East Carolina University in Greenville, NC. As previously reported, raw data was imported into Amira 5.4.0 Visualization and Volume Modeling Software (Visage Imaging, GmbH, Berlin, Germany) to enable visualization of images (Bae et al., 2011b; Perry et al., 2011; Tian et al., 2010a, 2010b, 2010c). This software includes a native Digital Imaging and

Communications in Medicine (DICOM) support program to ensure MRI data maintains the original anatomical geometry.

Three-dimensional MRI data re-sampling enabled visualization of midsagittal and oblique coronal images for each participant. Midsagittal images were identified and aligned with oblique coronal planes to ensure visualization of desired structures. Coronal plane image slices were available using the three-dimensional data at rest. Visualization of the midsagittal, axial, and oblique coronal image planes is provided in Figure 1. Cranial measures including distance between nasion and sella turcica, distance between basion and sella turcica, distance between opithsion and basion, nasion/sella turcica/basion angle, basion/sella turcica/opithsion angle, distance between the anterior border of the hard palate and basion, cranial length, and cranial width were obtained by measuring the midsagittal and oblique coronal image planes of each participant at rest (Table 4). Velopharyngeal measures of interest were obtained by measuring the midsagittal and coronal planes of each participant at rest and included hard palate width, hard palate height, hard palate length, distance from the posterior border of the hard palate to the canal of the incisive foramen, velar length, velar thickness, functional portion of the velum, velar knee to posterior pharyngeal wall, and pharyngeal depth (Table 5). These points of interest are presented in Figures 2 and 3. Oblique coronal images displayed the full sling of the levator muscle from the cranial base to middle of the velum. Linear measures of the levator muscle can be visualized in Figure 4. Static measurements of the levator muscle (Table 6) including distance between origin points, average muscle length, average angle of origin at the cranial base, average extravelar muscle length, intravelar segment length, and velar insertion distance were obtained by measuring the oblique coronal image plane of each participant at rest through

methods cited in previous literature (Bae et al., 2011b; Ettema et al., 2002; Ha et al., 2007; Perry et al., 2013).

Visualization of images during production of phonemes in "ampa" required steps to align the speech sample appropriately, clip the full video to one production of "ampa," and ensure correct determination of frames per phonemes. The full MRI video with aligned speech recording were imported into Adobe After Effects (Adobe After Effects CS5.5, v10.5) and clipped to one production of "ampa." In some cases, background noise of the MRI scanner interfered with visualization of the waveform of the speech task in Praat (Praat: Doing phonetics by computer, v5.3.53). In these cases, Camtasia Studio 7.0 (Camtasia Studio, v7.0) enabled removal of background noise to enable reliable determination of timing and selection of each phoneme involved in the speech sample. The sound file was analyzed through Praat to determine timing of phoneme production based on the waveform and formants. All imaging data were inspected to ensure that associated acoustic features were correctly identified. Phoneme productions were noted on the spectrogram according to the known acoustic features, and timing was confirmed by examining the associated image. Spectral analyses were included to ensure all phonemes and associated frames were accurately identified. The clipped video was analyzed in Adobe After Effects to identify frames corresponding with phonemes within the speech sound. After manual recording of frames associated with each speech sound within the speech task, full image sequences were exported as TIF image files labeled according to frame of the clipped MRI video. Frames at rest were identified through perceptual inspection of the full MRI video aimed at selection of a frame without any speech or swallowing movements when the velum was observed to rest on the base of the tongue. Full image sequences from the clipped MRI video were imported into Amira 5.4.0 as sequential TIF image files. Frames corresponding to

production of each phoneme and one frame of the participant at rest were measured based on manual recordings from spectral analyses and visual confirmation. This process was completed twice for each participant to establish measures for both the sagittal and oblique coronal planes of view. The oblique coronal image displaying the most cohesive levator sling during production of each phoneme of the speech sample was identified as described above.

Dynamic measures are described in Table 7. Velar measures of change in α angle, β angle, and velar stretch were obtained from the midsagittal image plane during production of each phoneme and compared to measures obtained from a rest image within the dynamic sequence. As displayed in Figure 5, α angle was measured as the angle formed at the intersection of a line drawn from the anterior borer of the hard palate to the posterior border of the hard palate and posteriorly to extend to the velar knee during production of each phoneme in the speech task. β angle was measured as the angle formed at the intersection of a line drawn from the posterior border of the hard palate to the velar knee and inferiorly to intersect with the uvula, as shown in Figure 6. This method for measuring β angle represents a slight modification from the original method for measuring β angle reported by Lipira and colleagues (2011). Previous research by Lipira et al. (2011) suggested change in α angle from rest to VP closure as an indicator of closure integrity and velar mobility, while a more notable change in β angle from rest to closure indicated a greater degree of velar bending at the approximate location of the levator muscle in the velar knee. Velar stretch was measured as the distance from the posterior border of the hard palate to the point of contact between the velar knee and posterior pharyngeal wall during VP closure. Measures of change in mean levator muscle length were obtained from the oblique coronal images corresponding to each phoneme in the speech sequence and compared to measures obtained from the rest image of the dynamic sequence.

Statistical Analysis

Differences in cranial, velopharyngeal, and levator muscle measures between the two groups at rest were analyzed using independent sample t-tests ($\alpha < 0.05$). Independent sample t-tests were also utilized to examine velar and levator measures during production of phonemes in "ampa" for each group. Parametric statistical analyses enabled quantitative analyses of measures between the two groups at rest and during production of "ampa." As the vowel sound "a" is produced twice during each production of "ampa," each was included as a separate production to examine effects of coarticulation and assimilation to surrounding phonemes. Sample sizes for both tests were limited (N=12, N=8), which prevented the benefit for adjusting for multiple statistical analyses.

Two investigators with experience in three-dimensional MRI data processing randomly selected data from 60% of participants approximately three months after initial determination of measurements to re-measure for reliability purposes. This procedure was completed for measures obtained at rest and angular measures obtained during speech production. Pearson product correlation was employed to obtain intra and inter-rater reliability measures.

Intra-rater reliability for static parameters of interest was relatively strong, ranging from $r = .84$ to $r = .99$. For participants in the cleft anatomy group, r values were lowest for measures of distance between the posterior border of the hard palate and posterior pharyngeal wall ($r = .91$) and distance between the velar knee and posterior pharyngeal wall ($r = .88$). Of participants in the normal anatomy group, r values were below .90 for measures of the posterior border of the hard palate to canal for incisive foramen ($r = .88$) and distance between basion and opithsion ($r = .84$). Intra-rater reliability for dynamic angular measures was also high, ranging from $r = .98$ to r

= .99. The range for the cleft anatomy group was r = .993 to r = .998, while the range for participants with normal anatomy was r = .98 to r = .99.

Inter-rater reliability for static parameters ranged from r = .63 to r = .99 for all participants. Reliability for static measures of adults with repaired cleft palate ranged from r = .63 to r = .99, while the range for adults with normal anatomy was r =.65 to r = .99. Static inter-rater reliability was greatest for measures of the cranium and velar length/thickness, while reliability was less consistent for other measures of the hard palate, velum, and levator muscle. Inter-rater reliability for dynamic measures ranged from r = .60 to r = .97. The range for the cleft anatomy group was r = .60 to r = .96, while the range for participants with normal anatomy was r = .76 to r = .97. Inter-rater reliability for dynamic measures was greatest for β angle measures (range: r = .88 to r = .97), and less consistent for α angle (range: r = .60 to r = .76).

CHAPTER 3: RESULTS

Static Rest Condition

Cranial measures. Cranial measures were obtained to determine if the participants showed similar overall cranial size. Table 8 displays means and standard deviations for cranial measures at rest for the two groups. Measures of opithsion to basion, facial height, and cranial length were slightly greater for adults with repaired cleft than those with normal anatomy, although these differences were not significant. Increased variability was also observed for cranial measures for the repaired cleft group, as indicated by elevated standard deviations. Overall, there was a non-significant difference in the cranial size between the two groups. Although nasion-sella-basion angle was not significantly different between groups, the posterior cranial base (sella turcica-basion-opithsion) showed a significant trend (p = .004) with adults with repaired cleft palate displaying a more acute angle (average: 128.6°, SD: 5.0) compared to those with normal anatomy (average: 140.6°, SD: 6.3). Cranial index measures were obtained through calculations previously described by Tian and Redett (2009) and Tian et al. (2010a). Cranial index was determined by dividing cranial length by cranial width. Cranial base index was determined by dividing the distance between the anterior border of the hard palate and basion by the distance between levator muscle origin sites. No significant differences were noted on either cranial index between the two groups.

Levator measures. The first hypothesis examined was to determine if there are differences in levator muscle and VP structure anatomy at rest between adults with repaired cleft palate (n=6) and adults with normal anatomy (n=6). Midsagittal and oblique coronal planes for selected participants from each group can be examined in Figures 7 and 8.

No significant differences between adults with repaired cleft and those with normal anatomy were noted for any measures of levator morphology at rest. Table 9 depicts group means for levator measures at rest for each study group. Average muscle length and angle of origin measures were similar across the two groups, although adults with repaired cleft palate exhibited a greater degree of variability across participants. Average extravelar muscle length and velar insertion distance were also fairly consistent across the two study groups. Length of the intravelar segment, or the curvilinear portion of the levator muscle within the velum, was also similar for each study group.

Although no significant differences in muscle measures were noted, qualitative differences can be appreciated between groups, particularly as it relates to the overall shape and cohesiveness of the levator sling. All participants with normal anatomy exhibited cohesive levator muscle slings with no midline separation. Adults with repaired cleft palate, on the other hand, exhibited variability between participants in separation of the levator muscle at its midline, as three to five were observed to exhibit a midline separation of muscle fibers within the velum. This midline separation of the levator muscle existed at the same location that musculus uvulae fibers were clearly identified in all normal participants. Adults with repaired cleft also exhibited variability between participants in the presence of musculus uvulae fibers. It was difficult to differentiate between a true midline separation of levator muscle fibers and atypically shaped musculus uvulae fibers in two of the cleft participants, as shown in one participant in Figure 9. These fibers were clearly absent in one out of six participants with repaired cleft. Participants with normal anatomy had visible musculus uvulae fibers at the midline of the levator, but the relative size varied. Three participants with normal anatomy exhibited a bulge along the dorsal surface of the velum into the nasopharynx, which may be caused by thicker musculus uvulae

fibers, while the other three adults with normal anatomy exhibited more broad/flat shaped musculus uvulae fibers that appeared to be intermingled with fibers of the levator muscle.

Some variation in levator bundle thickness was noted across adults with normal anatomy, but the general shape of the levator muscle appeared consistent in participants in this group. The levator muscle shape varied between participants with repaired cleft, with one displaying a "U-shaped" morphology, while two depicted more of a "V-shaped" levator sling. This variability in muscle configuration along its course was not observed in any participants in the normal anatomy group.

Velopharyngeal measures. Significant differences between adults with repaired cleft palate and those with normal anatomy were observed for measures of pharyngeal depth (normal: 20.9 mm +/- 2.5, cleft: 28.1 mm +/- 3.5, $p = .02$) and VP ratio (normal: 1.28 +/- 0.26, cleft: 0.85 +/- 0.18, $p = .008$). Velar length measures for adults with repaired cleft palate were less than for adults with normal anatomy; however, differences were not significant ($p = .08$). Distance between the velar knee and posterior pharyngeal wall was similar across the two groups, though adults with repaired cleft exhibited more variability between participants. Table 10 provides average results for VP measures at rest for each study group.

Visual inspection of midsagittal images at rest revealed increased variability in velar thickness along the length of the velum in the cleft group compared to all participants with normal anatomy. The velum was observed to exhibit consistent thickness throughout its length in three participants with repaired cleft, while other participants in this group demonstrated increased variability between participants. One participant revealed thickest velar appearance towards the uvula, while another depicted an atypical bulge projecting posteriorly at the approximate location of the velar knee with extremely thin tissue depicted more

posteriorly/inferiorly along the length of the velum. One participant demonstrated an anterior bulge of the posterior pharyngeal wall at the approximate location of VP closure. All participants with normal anatomy exhibited consistent velar thickness throughout the length of the velum, in agreement with previous reports (Ettema & Kuehn, 1994; Kuehn & Moon, 2005).

Palatal width was similar across the two groups, but palate height was significantly (p = .015) smaller in adults with repaired cleft palate (average: 8.7 mm, SD: 1.4) compared to normal anatomy (average: 12.1 mm, SD: 2.4). Pharyngeal depth, measured as the distance between the posterior border of the hard palate and the posterior pharyngeal wall, was significantly greater in adults with repaired cleft palate than those with normal anatomy (p = 0.02). Velopharyngeal (VP) ratio, as described previously by Hoopes, Dellon, Fabrikant, Edgerton, and Soliman (1969b) and Tian et al. (2010a), was calculated by dividing velar length by pharyngeal depth. VP ratio was 1.3 (SD: 0.3) in adults with normal anatomy, and 0.9 (SD: 0.2) in adults with repaired cleft palate (p = .008). This indicated a statistically significant difference in VP ratio between the two groups, as adults with repaired cleft palate exhibited overall smaller VP ratio values than those with normal anatomy. The fact that pharyngeal depth and VP ratio were significantly different across groups, but velar length and thickness were not, may indicate that measures of velar morphology might be significantly different between cleft and normal anatomy if the sample size were increased.

Speech Condition

The second study hypothesis aimed to examine if there are differences in VP function during speech production between adult participants with repaired cleft palate and those with normal anatomy. Head motion was excessive for two of the original 12 participants, which resulted in removal of four total (two cleft, two normal) datasets from dynamic data analyses.

Eight total datasets were analyzed during the speech condition (four adults with normal anatomy, four adults with repaired cleft palate). Dynamic measures of levator length change, α angle, β angle, and velar stretch were obtained across each phoneme during production of "ampa." These measures were obtained to reflect the degree of levator muscle contraction and extent of velar mobility, flexibility, and stretch during phonation of speech sounds. Results for all dynamic measures for each group are provided in Tables 11 - 15.

Levator measures. Measures of change in mean levator muscle length were obtained from the oblique coronal images corresponding to each phoneme in the speech sequence and compared to measures obtained from the rest image of the dynamic sequence. These percent changes were examined relative to each participant's original levator length value, as obtained from rest images. Measures of percent change and applied dynamic measurements of the levator muscle during speech are provided in Tables 11 and 12.

No statistically significant differences in percent change of the levator muscle were observed for any of the phonemes within "ampa" between adults with repaired cleft palate and those with normal anatomy. Changes in levator length during speech production can be visualized in Figures 10 – 15. Adults with normal anatomy exhibited a 1.7% decrease in levator length during production of the first speech task, while those with repaired cleft palate exhibited a decrease by 7.3%. A 1.5% decrease in levator length was observed for adults with normal anatomy during production of "m," but adults with repaired cleft exhibited a 0.8% increase in levator length during production of the nasal phoneme. Both groups exhibited a decrease in levator length from rest to production of the third phoneme, "p," with a 20.8% reduction for adults with normal anatomy and 11.6% reduction for those with repaired cleft palate. A similar pattern of levator length change was observed during production of the final phoneme, "a," with

16.2% and 10.8% reductions in levator length for adults with normal anatomy and those with repaired cleft palate, respectively. Although mean values appear to vary between the two groups, the lack of statistical significance is likely related to the great degree of variability noted within both study groups and small sample size.

In the oblique coronal image plane, a consistent pattern of levator movement during speech was observed for most participants in this investigation. Visualization of the VP mechanism and levator muscle in the oblique coronal plane for one participant with normal anatomy and one with repaired cleft palate is provided in Figure 16. However, variability within and between groups was observed. Three participants with normal anatomy displayed minimal levator shortening (contraction) during the first task (first "a" in "ampa"), while one participant did not exhibit any movement of the levator muscle from rest to production of the first phoneme in the speech task. Variability in levator functioning during production of "ampa" was also observed for participants with repaired cleft palate. The levator muscle exhibited little to no contraction from rest to production of the first speech task ("a" in "ampa") for three participants with repaired cleft palate. All participants with normal anatomy revealed visible relaxation and lengthening of the levator muscular sling during production of the nasal "m." Levator length appeared greatest during production of nasal phoneme "m," and contracted to exhibit the shortest visible configuration during production of the oral syllable, "pa," for three participants with repaired cleft. The fourth participant in the repaired cleft group did not exhibit this pattern during speech production, instead exhibiting variable levator function across repetitions of the speech task and inconsistent incomplete VP contact without the presence of perceptual hypernasality.

Velopharyngeal measures. For all adults with normal anatomy, VP closure during speech involved contact of the midportion of the velum against the posterior pharyngeal wall. Adults with repaired cleft palate demonstrated more variability in place of contact between the velum and posterior pharyngeal wall during closure. Figure 17 provides visualization of levator and velar motion during production of "ampa" for one participant with normal anatomy. Most participants with normal anatomy demonstrated slight elevation of the velum to approximate the posterior pharyngeal wall during the first task in "ampa," while adults with repaired cleft palate exhibited variability in velar motion during this and the other speech tasks. One participant with normal anatomy displayed slight lowering of the velum during production of the entire first nasal syllable ("am"), and perceptual analyses revealed production as similar to production of syllabic "m." During production of nasal "m," the extent of flexion at the velar knee during velar lowering varied across adults with normal anatomy more than during production of the oral phonemes in the speech task. Some maintained an anticipatory position for VP closure by maintaining a state of flexion at the approximate location of the medial portion of the levator, while others depicted more of a relaxed position during velar lowering. Rapid and forceful posterior and superior movement of the velum towards the posterior pharyngeal wall occurred during production of the third and fourth tasks ("pa") for all adults with normal anatomy.

Two participants with repaired cleft exhibited lowering of the velum during production of the first and second tasks ("am") and clear contact of the velar knee bend with the posterior pharyngeal wall during the third and fourth tasks ("pa"). These two participants revealed the dorsal portion of the velum beyond the velar knee to extend inferiorly approximating or resting against the posterior pharyngeal wall during all speech tasks. The remaining two adults with repaired cleft palate presented increased variability in velar motion during production of "ampa."

One participant with repaired cleft palate utilized a glottal stop during production of "p" in the speech stimuli, indicated by incomplete/inconsistent closure of the VP port, posterior movement of the tongue towards the posterior pharyngeal wall, and simultaneous bilabial closure during production of the plosive "p."

Changes in α angle were obtained from the midsagittal image plane during production of each phoneme and compared to measures obtained from a rest image within the dynamic sequence. As displayed in Table 13, results are reported in percent of angular change from rest to production of each phoneme in "ampa." A significant difference ($p = .007$) between groups was observed for α angle during production of the first task (initial "a" in "ampa"), as adults with normal anatomy exhibited a 0.8% increase in α angle, while adults with repaired cleft exhibited a 4.3% decrease. Both groups exhibited an average increase in α angle during production of the nasal phoneme "m." During production of "p," adults with repaired cleft palate exhibited a 6.1% decrease in α angle, indicating a statistically significant difference ($p = .006$) from the 0.5% increase observed in adults with normal anatomy. This difference remained significant ($p < .001$) in analyses of percent change in α angle during production of the final phoneme, "a," as adults with repaired cleft exhibited a 5.8% decrease in α angle from rest to production of the task, while those with normal anatomy exhibited a 0.5% increase.

Changes in β angle were obtained consistent with procedures described above and are provided in Table 14. Results are reported in percent of angular change from rest to production of each phoneme in "ampa." Adults with normal anatomy exhibited an average decrease in β angle by 7.0% from rest to production of the first speech task, which is significantly less than the average decrease of 11.4% observed in adults with repaired cleft palate ($p = .034$). During production of "m," adults with normal anatomy exhibited an average 13.2% increase in β angle

compared to a significantly smaller increase of 6.1% for adults with repaired cleft palate (p = .022). During production of "p," both groups exhibited a similar degree of reduction in β angle compared to rest. During the final "a" in the sample, the normal anatomy group exhibited a significantly greater degree of reduction in β beta angle compared to those with repaired cleft (p = .045) with averages of -20.3% and -14.1%, respectively.

Changes in degree of velar stretch were obtained from the midsagittal image plane during production of each phoneme and compared to measures obtained from a rest image within the dynamic sequence. Group means are provided in Table 15. No statistically significant differences in percent of change in velar stretch were observed between the two groups during production of any phoneme within the speech sample. Both groups exhibited average increases in velar stretch from rest to production of the first phoneme, "a," third phoneme "p," and final phoneme "a," with average decreases in velar stretch noted during production of nasal phoneme, "m." The greatest amount of velar stretch was noted for phoneme "p" (normal: + 55.6%, cleft: +30.4%) with the least amount of velar stretch observed during production of "m" (normal: -10.1%, cleft: -7.9%) for both groups of participants.

CHAPTER 4: DISCUSSION

Rest Condition

Similar to previous findings (Sandham & Cheng, 1988) participants with repaired cleft palate did not exhibit any difference in nasion-sella-basion angle, a measure of the anterior angle of the cranial base, compared to adults with normal anatomy in the present investigation. The posterior cranial base angle, established as the smaller angle formed at the intersection of sella-turcica to basion and basion to opithsion linear measures, was significantly (p = .004) more acute in participants with repaired cleft palate (average: 128.6°, SD: 5.0) compared to those with normal anatomy (average: 140.6°, SD: 6.3). Previous reports suggest cervical spine abnormalities to be more common in individuals with cleft palate compared to those with normal anatomy (Hoenig & Schoener, 1992; Horswell, 1991; Sandham, 1986; Uğar & Semb, 2001). It is possible that the difference in posterior cranial base angle may be caused by cervical abnormalities among the participants with repaired cleft palate; however, measures of cervical spine abnormalities were not within the scope of this research study. Additionally, no subjects reported a history of syndromes; however, it was not determined if each individual had genetic testing to confirm the absence of a syndrome.

Levator measures. No significant differences were observed between participants with repaired cleft and those with normal anatomy in measures of the levator muscle at rest. The lack of statistically significant differences observed may be related to low sample size (N=12) and variability within each study group. A power analyses performed as part of a large-scale study on adult VP anatomy (Perry, Kuehn, Sutton, Gamage, & Fang, in press) determined that 14 participants per study group is necessary for establishing statistical significance (at least 80% power, $\alpha = 0.05$). Only six participants were included within each study group in the present

investigation. Although levator muscle measures have not been shown to vary significantly based on race, significant differences between males and females have been reported for measures of the levator muscle and other structures in the VP region (Bae et al., 2011b; McKerns & Bzoch, 1970; Perry et al., in press). Ettema et al. (2002) did not report significant differences in levator length between males and females, but may have been limited by a smaller sample size. In the current investigation, variability within each study group in sex could account for the lack of significant differences observed between cleft and normal anatomy.

Adults with normal anatomy exhibited an average levator length of 45.3 mm (SD: 3.5), and those with repaired cleft exhibited slightly a slightly smaller average length of 44.4 mm (SD: 5.0). Previous research has documented decreased levator length in individuals with repaired cleft palate (Ha et al., 2007; Tian et al., 2010c). Ha et al. (2007) reported an average levator length of 40.0 mm in adult males with repaired cleft palate compared to an average of 46.0 mm for adults with normal anatomy previously reported by Ettema et al. (2002). Other investigators have reported average levator muscle length in adults with normal anatomy as 32.6 mm (SD: 2.8; Tian & Redett, 2009), 42.5 mm (SD: 4.73; Bae et al., 2011b), and 47.5 mm (Perry et al., 2013). In the current study, levator length ranged from 34.8 to 49.1 mm for adults with repaired cleft palate and 42.0 to 48.7 mm for adults with normal anatomy. Previous research also reported large ranges in levator length across adults with normal anatomy, with a range of 37.6-50.8 mm reported by Bae et al. (2011b) and a range of 41.7-52.9 mm reported by Perry et al. (2013). Ha et al. (2007) reported a range in average levator length of 38.0-44.0 mm for three adult males with repaired cleft palate, which was less variable than the range of 34.8-49.1 mm reported in the current study. This difference may be related to differences in sample sizes between Ha et al.

(2007), which included three participants, and the six participants with repaired cleft examined in the current investigation. Future studies should include larger sample sizes.

Adults with normal anatomy consistently exhibited a cohesive sling of the levator muscle while three participants in the repaired cleft group exhibited midline separation of the levator muscle. This is in agreement with previous research by Kuehn and colleagues (2001; 2004), who reported insufficient cohesion of the medial levator muscle bundles within the velum following cleft repair surgeries. Ha et al. (2007) also reported discontinuity in the levator muscle at midline in four adult males with repaired cleft palate.

Levator configuration and morphology was visibly different and more variable within the repaired cleft palate group than for adults with normal anatomy. Ha et al. (2007) reported levator configuration in adults with repaired cleft palate did not form a gradual curve into the velum as observed in normal anatomy, but instead projected inferiorly before projecting medially at sharp angles. These differences in muscle configuration were not observed in the normal anatomy group. Lindman, Paulin, and Stal (2001) observed increased variability in levator configuration and size in infants with cleft. It is possible that surgical intervention for cleft palate affects development of the levator muscle with age, which may provide one possible explanation for the variability observed between participants in the repaired cleft group.

It has been previously suggested that linear measures of the levator muscle (muscle length, distance between origin points) obtained through MRI do not accurately portray the complex and three-dimensional shape of the levator muscle along its course from the cranial base to the velum (Perry et al., 2013). It is possible that linear measures of the levator reported in this investigation oversimplify the muscle and do not allow for consideration of muscle form, diameter, or circumference in comparisons between adult participants with repaired cleft and

those with normal anatomy. Perry et al. (2013) proposed a method for assessing these morphological differences using a novel method for calculating muscle diameter and circumference at various points along its course. This method may provide a more accurate representation of the complex nature of the levator muscle and may enable more reliable examination of differences between cleft and normal anatomy. Given the qualitative differences observed among participants in this study, future studies should employ similar methods to examine specific differences in levator morphology and configuration between cleft and normal anatomy.

Velopharyngeal measures. Adults with repaired cleft exhibited greater average measures of pharyngeal depth and smaller average VP ratio than participants with normal anatomy. Velopharyngeal (VP) ratio was significantly greater ($p = .008$) for adults with normal anatomy (1.28) than those with repaired cleft palate (0.85). Similar to measures reported here, previous reports of VP ratio in adults with normal anatomy have been reported ranging from 1.2 to 1.43. Subtelny (1957) reported values that enabled calculation of approximate VP ratio of 1.43 for adults with normal anatomy. Tian et al. (2010a) reported an average VP ratio of 1.23 for adults with normal anatomy. Hoopes et al. (1969b) reported individuals with normal anatomy exhibited an average VP ratio of 1.35, while those with insufficient VP closure exhibited an average VP ratio of 1.05. Tian et al. (2010c) reported children with normal anatomy to exhibit an average VP ratio of 1.5, greater than average ratios of 1.1 and 1.0 in children with repaired cleft palate. Satoh et al. (2002) reported average VP ratio of 1.2 for 18 year olds with normal anatomy and did not observe any significant differences between participants with normal anatomy and those with repaired cleft in a cross-sectional study design from 4-18 years. The

observed difference in VP ratio between groups is related to the measures of pharyngeal depth and velar length.

Many reports from previous investigations have documented significantly shorter velar length measures in children and adults with repaired cleft palate compared to normal anatomy (Akgüner et al., 1998; Coccaro, Subtelny, & Pruzansky, 1962; Özgür et al., 2000; Satoh et al., 2002). Tian et al. (2010c) suggested shorter velar length in repaired cleft compared to normal anatomy might be related to more scar tissue formation in the velum following cleft palate repair surgery. Graber et al. (1959) reported measures of velar length in adults with normal anatomy ranging from 32.0 mm to 49.0 mm. Bzoch (1968) documented an average velar length of 33.0 mm in male adults with normal anatomy. Ettema and Kuehn (1994) reported an average velar length of 38.3 mm in adults with normal anatomy with a variable range of 30.9 to 46.2 mm. More recently, Satoh et al. (2002) reported an average velar length of 25.8 mm (SD: 2.8) for young adults with repaired cleft palate and average length of 32.4 mm (SD: 3.2) for young adults with normal anatomy. Similar to findings of Satoh et al. (2002), average velar length for adults with repaired cleft palate was 24.1 mm (SD: 6.3) and 30.1 mm (SD: 4.2) for adults with normal anatomy in the current investigation. However, the difference between groups was nonsignificant (p = .08), and each group demonstrated a high degree of variability between participants. Increased variability in velar length in children with repaired cleft has been previously reported (Tian et al., 2010c). Perry et al. (in press) demonstrated significant differences by race and sex for measures of velar length and thickness. It is likely that the limited sample size and heterogeneity of the group by race and sex may be related to the lack of statistical significance. Future studies are needed to investigate the differences between cleft and non-cleft anatomy using larger and more homogenous sample sizes.

Pharyngeal depth was determined to be significantly greater in adults with repaired cleft palate than those with normal anatomy (p = .02). Tian et al. (2010c) reported significantly greater pharyngeal depth in children with repaired cleft palate in comparison to children with normal anatomy. Previous investigators have reported average pharyngeal depth measures for adults with normal anatomy ranging from 17.5 to 26.7 mm (Bae et al., 2011b; Perry et al., 2014; Satoh et al., 2002; Tian & Redett, 2009; Tian et al., 2010a). In contrast to findings of the present investigation, Satoh et al. (2002) reported an average pharyngeal depth of 21.1 mm (SD: 3.2) for young adults with repaired cleft palate, which was significantly less than the reported average of 26.7 mm (SD: 2.6) in young adults with normal anatomy.

It is likely that the shorter hard palate observed in participants with repaired cleft palate contributes to the larger pharyngeal depth measures when compared to non-cleft anatomy. Normative values for palate length (anterior to posterior length of the hard palate) were previously reported as 52.9 mm (SD: 5.3, Tian & Redett, 2009), 60.6 mm (SD: 5.7; Perry et al., 2014), 52.4 mm (SD: 4.8; Bae et al., 2011b), and 48.4 mm (SD: 4.4; Tian et al., 2010a) in adults with normal anatomy. Tian et al. (2010c) reported greater standard deviation from the mean in groups of children with repaired cleft palate than children with normal anatomy. Palate length was also more variable across adult participants in the repaired cleft group in this investigation. Observations of shorter hard palate length in samples of children with repaired cleft compared to those with normal anatomy were previously reported (Tian et al., 2010c; Zajac, Cevidanes, Shah, & Haley, 2012). In the present investigation, adults in the normal anatomy group exhibited an average palate length of 56.3 mm (SD: 1.8). This measure was significantly (p = .025) longer than the average palate length of 51.7 mm (SD: 3.9) observed for adults with repaired cleft palate.

Previous investigators have provided evidence for decreased maxillary dimensions in individuals with repaired cleft palate compared to those with normal anatomy (Crabb & Foster, 1977; Shibaski & Ross, 1969; Tian et al., 2010c; Wada et al., 1997). Fusion of the hard palate is disrupted during embryological development in individuals with repaired cleft palate, and surgical correction aims to connect mucoperiosteal tissue in the midline to enable growth of bone to correct the cleft. Ishikawa et al. (1998) suggested scar tissue formation in the region of the hard palate likely contributes to constricted maxillary growth in individuals with repaired cleft palate. Previous investigators have reported worse craniofacial morphology in individuals with repaired cleft palate compared to a more typical pattern of growth observed in age-matched individuals with unoperated cleft palate (Khanna, Tikku, & Wadhwa, 2012; Law & Fulton, 1959). The significantly shorter palate length observed in adults with repaired cleft compared to those with normal anatomy may suggest abnormal development of the hard palate following cleft palate repair surgery.

Additionally, two adults in the repaired cleft group also exhibited a lack of posterior extension of the posterior border of the hard palate, which differed from the more typical anterior-posterior placement of the posterior border of the hard palate in the remaining four adults in this group and all adults with normal anatomy. Tian et al. (2010c) reported similar findings in groups of children with repaired cleft palate. The variability in degree of posterior extension of the hard palate observed between participants in the repaired cleft group was not observed in participants with normal anatomy. This differs from previous reports by Satoh et al. (2002) and Wada et al. (1997), who observed the posterior maxillary point to project further posterior and superiorly in individuals with repaired cleft compared to controls with normal anatomy. These investigations, however, were completed using lateral cephalograms, studied

children through teenage years, and focused on individuals with repaired unilateral cleft lip and palate. Shibaski and Ross (1969) reported children with repaired cleft exhibit overall decreased growth in length and height of the maxilla in comparison to children with normal anatomy.

Measures of hard palate height were significantly greater in adults with normal anatomy compared to those with repaired cleft palate. Values obtained in the present study on normal adults are consistent with palate height measures reported by Yunusova et al. (2012), who reported an average palate height of 13.5 mm (SD: 2.5) for adult males with normal anatomy. Perry et al. (2014) reported a smaller average palate height for ten adult males with normal anatomy (average: 9.3 mm, SD: 3.1) than the present average of 12.1 mm for the normal anatomy group; however, the investigators reported a variable range across participants (5.4-14.6 mm). The normal anatomy group in this investigation also demonstrated a high degree of variability across participants (range: 8.1-14.4 mm). Hard palate height has been previously observed to vary significantly between males and females (Perry et al., in press). Differences in hard palate and cranial morphology in individuals with different types of cleft lip/palate have been previously reported (Bishara et al., 1976). Given the inclusion of male and female participants with different types of cleft and different methods of surgical correction in the present investigation, variability each group may have impacted statistical findings.

Previous investigators have reported shorter palatal and alveolar heights in children and adults with a history of cleft palate compared to those with normal anatomy (Crabb & Foster, 1977; Wada & Miyazaki, 1975; Zajac et al., 2012). After cleft palate repair surgery, mucoperiosteal flaps tethered in the midline develop into bone. During this time, the dental arch may develop abnormally, such as in a way that is more likely to collapse (Reichert, 1970). This abnormal development of the arch and potential collapse might explain shorter palate height

measures observed for participants with repaired cleft palate in the present investigation. Significantly smaller measures of palate height in adult participants with repaired cleft palate compared to those with normal anatomy further support the possibility of abnormal development of the hard palate following cleft palate repair surgery. Zajac et al. (2012) suggested that dental arch variations might factor into later development of abnormal articulation. Maxillary and VP variations reported in the current investigation may play a role in causing aberrant speech patterns, or compensatory misarticulations, frequently observed in individuals with repaired cleft palate. Future investigations should examine these variations and the relationship between these variations and aberrant speech patterns in children with repaired cleft palate.

Speech Condition

Differences in VP functioning were observed between participants with repaired cleft palate and those with normal anatomy. Adults with normal anatomy exhibited more consistent/predictable VP movements during speech production, while those with repaired cleft palate exhibited inconsistent VP function and within-group variability. However, few significant differences were observed between the groups during production of the speech sequence, "ampa."

Levator measures. No statistically significant differences were observed between groups for percent of levator change across the speech task; however, mean values appeared to vary somewhat between the two groups across production of each phoneme. Small sample size and high amount of variability within and between each group likely contributed to the lack of significant differences reported between the two groups. Although no levator muscle differences were statistically provided, angles during speech production and observation of MRI movies revealed differences in overall functioning of the VP mechanism for speech between adults with

repaired cleft and those with normal anatomy. Findings of Warren, Dalston, and Mayo (1993) suggest differences in timing and duration of VP closure to cause perceptual differences in the speech of individuals with repaired cleft palate without obvious VP insufficiency. As the levator is known to be the primary muscle involved in VP closure, this study provides preliminary evidence that although the muscle may appear similar in adults, the use of structures and/or other muscles involved may vary between repaired cleft and normal anatomy.

Participants with normal anatomy exhibited a consistent pattern of levator movement during speech production, while those in the repaired cleft group exhibited more variability. Visual inspection of MRI movies revealed noticeable variation in shape, position, and degree of levator movement during speech production for adults with repaired cleft palate. One participant in the repaired cleft group did not follow any notable pattern and exhibited inconsistent VP function/dysfunction without the presence of perceptual hypernasality. Upon further inspection, this participant was noted to produce "p" phonemes inconsistently as glottal stops with simultaneous bilabial lip closure.

The majority of previously reported measures of change in levator length during speech production reflect levator length during sustained phonation of speech sounds. Because the MRI protocol employed in present investigation enabled obtainment of quantitative values during dynamic speech production, the current findings may be difficult to interpret/compare to previous reports. For adults with normal anatomy, levator length was observed to shorten by 1.7% during production of the initial "a," by 1.5% during production of "m," by 20.8% during production of "p," and by 16.2% during production of the final phoneme "a." Perry et al. (2014) reported percent changes in levator muscle during real-time speech production of "ansa" for ten adults with normal anatomy. The investigators documented a 14.0% shortening of the levator

during “a,” 5.0% shortening during “n,” 13.0% shortening during “s,” and 16.0% shortening during final “a” for these participants. The decreased degree of levator contraction observed in the present investigation and by Perry et al. (2014) during the initial “a” compared to the final “a” suggests anticipatory nasal positioning of the levator muscle during production of first “a” in “ansa.”

During production of the first speech task in “ampa,” the majority of participants with normal anatomy exhibited slight shortening of the levator, while the majority of participants in the repaired cleft group displayed no/little movement during production of the initial “a.” One participant with normal anatomy also exhibited little to no movement of the levator during production of this phoneme, which may be related to decreased activation of the levator muscle previously reported during production of open vowels, particularly when preceding a nasal phoneme (Bell-Berti, 1976; Kuehn & Moon, 1998). All participants with normal anatomy and three of the four participants with repaired cleft displayed longest levator muscle length during production of the nasal phoneme, “m.” In previous studies, longest levator length measures also occurred during nasal sounds (Ettema et al., 2002; Ha et al., 2007; Perry et al., 2014). Levator length was shortest, indicated by a greater degree of negative percent change, during production of “p” and “a” in the second syllable for both groups of participants. All participants with normal anatomy exhibited visible levator muscle contraction during production of phonemes in “pa,” as the levator was observed to flatten into a bar-like configuration in the midline. Pigott (1969) also observed tightening of levator sling into a bar during contraction for speech in participants with normal anatomy. This consistent muscle configuration was not observed in the repaired cleft group, although three of these participants also exhibited shortest levator muscle lengths during production of the two phonemes in the oral syllable.

The degree of change in levator length from rest to speech production has been observed to vary across normal and cleft anatomy. In the present investigation, levator length changes during speech production differed nonsignificantly between adults with repaired cleft and those with normal anatomy. Ha et al. (2007) and Ettema et al. (2002) found that levator length values were largest at rest, then decreased for production of nasal consonants, low vowels, high vowels, and fricative consonants. Ettema et al. (2002) reported a 2% increase in levator length from rest to sustained production of "m" for participants with normal anatomy, while Ha et al. (2007) did not observe any change in levator length from rest to sustained production of "m" in four adults with repaired cleft palate. Adults with normal anatomy and those with repaired cleft palate in these investigations exhibited similar degrees of levator shortening during sustained production of vowel "a." Ha et al. (2007) determined the average degree of change in levator length for adult participants with repaired cleft palate was 17.1% shortening from rest to production of fricatives, which is slightly lower than the 19.8% reduction reported for adults with normal anatomy by Ettema et al. (2002). Ha et al. (2007) suggested decreased levator muscle contractility in adults with repaired cleft palate compared to those with normal anatomy based on these findings. In agreement with Ha et al. (2007), adults with normal anatomy in the current investigation exhibited a maximum reduction in levator length by 20.8%, while those with repaired cleft demonstrated a maximum reduction of 11.6%.

Velopharyngeal measures. Visual inspection of dynamic data for adults with normal anatomy revealed predictable and consistent movements of the VP mechanism during speech production, with some variability between individuals. Individual variability in VP valving during speech production has been documented and described in previous investigations (Graber et al., 1959; Kuehn & Moon, 1998; McGowan et al., 1992).

Most participants with normal anatomy exhibited approximation of the velum towards the posterior pharyngeal wall during task one: the initial "a" in "ampa," while one did not exhibit any velar elevation until production of "pa." This observation may indicate normal nasalization of vowels produced immediately before nasal phonemes.

Participants with normal anatomy also exhibited variability in the degree of velar bending demonstrated during production of nasal phoneme "m." It is generally accepted that nasal phonemes are produced with the velum lowered, and levator muscle in a relaxed state compared to production of oral phonemes. However, some participants with normal anatomy exhibited a degree of continued bending of the velum at the velar knee during production of "m," indicating the levator muscle maintained its contracted state despite allowing air to resonate through the nasal cavity. Graber et al. (1959) reported a close-anticipatory velar position during production of "m," rather than a fully lowered configuration consistently across all participants. The investigators described the velar position during production of "m" to resemble closure more than a rest position and reported a high degree of variability between participants in the nature of velar physiology during production of nasal phonemes; however, the authors reported consistent observation of some degree of superior and posterior motion of the velum during production of nasal phonemes. McGowan et al. (1992) reported consistent observations of the velum in a lowered position, approximating its position at rest, for all participants with normal anatomy during production of nasal phoneme, "m," while all exhibited consistent bending of the velum during elevation. It is likely that McGowan and colleagues were unable to visualize effects of coarticulation, as each participant produced each phoneme during sustained phonation of 6 seconds per sound.

Previous research also described coarticulatory effects of nasal consonants on preceding vowels (Bell-Berti & Krakow, 1990; Kuehn, 1976; Kuehn & Moon, 1998; Moll, 1962; Moon, Kuehn, & Huisman, 1994a). Moon et al. (1994a) observed consistent incomplete VP closure across all participants with normal resonance during production of vowels adjacent to nasal phonemes. Moll (1962) observed insufficient VP closure in all participants during production of vowels in nasal syllables. Kuehn and Moon (1998) observed increased VP closure for oral consonants occurring immediately after a nasal consonant compared to oral consonants occurring directly before these nasal phonemes.

Results of previous studies have indicated variability in VP closure during production of the vowel "a" compared to other vowels and oral consonants. Hagerty, Hill, Pettit, and Kane (1958) reported only half of participants with normal anatomy exhibited full VP closure during production of "a," but all exhibited full closure during "s." Previous research has provided evidence for an overall lower velar position during syllables containing vowel "a" in comparison to those containing higher vowels such as /i/ and /u/ (Bzoch, 1968; Moll, 1962).

Visualization of 3D MRI movies revealed consistent forceful posterior-superior movement of the velum during production of the third and fourth tasks ("pa") of the speech sequence for all participants with normal anatomy. This corresponds to earlier findings of VP closure during production of plosive sounds (Pigott, 1969). Pigott (1969) documented most forceful VP closure during production of plosives and inconsistent VP closure during production of vowel sounds.

Participants with repaired cleft exhibited greater variability in velar motion during VP closure. Özgür et al. (2000) also reported variability in velar motion during speech production of individuals with repaired cleft palate through descriptions of shorter velar length and restricted

degree of velar motion in these individuals compared to those with normal anatomy. McGowan et al. (1992) observed complete VP closure and typical velar range of motion in four participants with repaired cleft with some variability in velar motion/morphology during sustained phonation of speech sounds. McGowan et al. (1992) reported that the shape of the velum did not change significantly from its relaxed state to its elevated state in these participants, but maintained a straight/flat appearance regardless of muscular contraction. The investigators hypothesized this reduced amount of bending/flexion of the velum during velar elevation could be related to results of surgical scarring. Kuehn and Moon (1998) suggested individuals with scarring from surgical repair of a cleft may demonstrate reduced flexibility/versatility in velar motion compared to those with normal anatomy, indicating these individuals may exhibit more constant degrees of VP closure force related to overall reduced range of motion. The authors further suggest a compromised position between fully lowered and fully elevated as evidence of velar impairment from scar tissue.

Observations of VP functioning during speech production provided insights into velar physiology in individuals with repaired cleft palate. Two participants with repaired cleft demonstrated visible lowering of the velum during production of the nasal syllable comprised of the first and second tasks in "ampa." These participants also displayed contact of the velar knee with the posterior pharyngeal wall during production of the third and fourth speech tasks, but contact was made at a dorsal point on the velum, rather than along the mid-portion of the velum, as observed in all participants with normal anatomy. Satoh, Wada, Tachimura, Sakoda, and Shiba (1999) also reported differences in point of velar contact along the posterior pharyngeal wall during VP closure between individuals with repaired cleft and those with normal anatomy. A high degree of variability between participants and inconsistencies in VP function within each

participant's speech production was noted for adults with repaired cleft palate. Kuehn and Moon (1998) measured activity of the levator muscle during speech production and described the process involved in VP closure for speech as flexible and complicated. It is possible that the interaction of other muscles involved in VP functioning and the levator muscle is different in repaired cleft anatomy than in normal anatomy. Seaver and Kuehn (1980) discussed the influence of the palatopharyngeus muscle on precise positioning of the velum during velar elevation. Perhaps the interaction of the palatopharyngeus and levator muscles in adults with repaired cleft plays a role in the greater degree of inconsistencies observed in each of the participants with repaired cleft. Shinagawa et al. (2005) suggested increased posterior movement of the tongue and superior/anterior projection posterior pharyngeal wall with no visible VP closure during speech production could be related to increased activity of the palatopharyngeus and palatoglossus muscles caused by decreased activity of the levator muscle in one individual with repaired cleft palate.

The α angle was measured as the angle at the intersection of a line drawn from the anterior nasal spine to the posterior border of the hard palate and posteriorly to extend to the level of the velar knee during production of individual phonemes (Figure 5). Significant differences between groups were observed during production of the first, third, and fourth tasks in the speech sequence, "ampa." Changes in α angle indicate the integrity of VP closure and degree of velar mobility. In other words, as α angle decreases, velar elevation increases. Therefore, α angle would be expected to decrease according to height of velar knee necessary for VP closure during production of each speech sound. Kuehn and Moon (1998) suggested that velar elevation is correlated to the degree of VP closure during production of vowels, which is

less during production of low vowels such as the "a" phonemes, compared to high vowels (e.g., /i/ or "eee").

As α angle increased minimally during production of all oral phonemes for adults with normal anatomy, these individuals did not require extensive velar elevation in order to achieve VP closure for these speech sounds. Adults with repaired cleft exhibited more significant decreases in α angle measures during production of oral phonemes than the normal anatomy group, suggesting participants with repaired cleft required more velar elevation to achieve VP closure than those with normal anatomy. During production of nasal "m," both groups exhibited an average increase in α angle, indicating the velar knee lowered to a degree from its rest state to production of the nasal syllable.

β angle was measured as the angle formed at the intersection of a line extending from the posterior border of the hard palate to the velar knee and inferiorly to intersect with the uvula (Figure 6). The method to obtaining β angle in the present investigation is a slight modification from a previous investigation by Lipira and colleagues (2011) that provides a more reliable method to examining the degree of flexion of the velum. Significant differences between groups were noted during production of the first, second, and fourth task in the speech sequence, "ampa." β angle is considered to represent the degree of velar flexibility, or the amount of bending of the velum at the approximate location of the levator muscle sling. Larger measures of β angle indicate more bending of the velum at the velar knee. Adults with repaired cleft exhibited somewhat greater bending during the first task, smaller degrees of flexion during the second task, and a reduced degree of bending during the third and fourth tasks than what was observed in adults with normal anatomy.

No significant differences were noted in percent change of velar stretch during production of "ampa" between the two groups; however, the velum was more variable in appearance and exhibited more gross and uncoordinated movements in participants with repaired cleft compared to the consistent appearance and fine/discrete velar movements observed in all participants with normal anatomy. Adults with normal anatomy demonstrated maximum velar shortening of 10.1% from rest to production of nasal "m," which indicates a greater degree of shortening for these participants than the maximum velar shortening of 7.9% observed for participants with repaired cleft palate. Bzoch (1968) cited a notable increase in velar length from rest to functioning during speech production (49.0% increase) in adult male speakers. Graber et al. (1959) also reported a large (approximately 40.0-43.0%) increase in length of the velum from rest to function during speech in normal speakers. A similar pattern was observed for maximum increase in velar length during production of phoneme "p." During production of "p," adults with normal anatomy exhibited lengthening of the velum by 55.6%, which is a greater degree of lengthening than the 30.4% exhibited by participants with repaired cleft palate.

Clinical Implications

The present investigation demonstrates a successful method of visualization with potential clinical utility given continued technological advancements in MRI. In general, additional research is necessary to improve the current understanding of dynamic muscle and soft tissue movements involved in VP function for speech production in normal and cleft anatomy. Increasing this knowledge base will facilitate further understanding of differences in velar positioning during speech and the impact of these dynamic positions on oral to nasal resonance during speech production. Continued advancements in technology and focus on improving image quality in dynamic MRI will facilitate future research in this area. Research

into the timing, coordination, and general structural movements of the muscles and soft tissues involved in VP closure may provide insight into perceptual differences of speech/resonance between normal speakers and those with repaired cleft without obvious hypernasality. This can be achieved with frame-by-frame analyses of MRI data from multiple planes during connected speech.

Continued evaluation of post-surgical outcomes in short and long terms may contribute to a better understanding of the effects of various types of cleft palate repair surgeries on the functioning of muscles and structures important in VP function for speech. Related to surgical outcomes, future investigations should examine the effects of scar tissue from palate repair surgery on VP functioning, as there is limited research on how scar tissue in this region impacts overall physiology after recovery.

Limitations of Study

Given the limited number of participants in the present investigation, all statistical findings must be interpreted with caution. These findings are specific to the participants examined in the present study and do not provide enough power for application to the general population. Participants in this investigation repeated the speech task approximately 15 times each during dynamic data acquisition. It is possible that repeated speech tasks such as this do not depict the true physiology involved in spontaneous conversational speech. A difference in average BMI was noted between the two groups of participants, as adults with repaired cleft palate exhibited an average BMI of 28.48 (in the pre-obesity range), much higher than the average 22.25 BMI (normal range) in the normal anatomy group.

There is limited research on the risk of obesity in adults with a history of craniofacial anomalies, but other factors that may lead to an increased weight/BMI in this population have

been discussed previously. Individuals born with craniofacial anomalies, such as cleft lip/palate, are at a higher risk for developing health and social related problems with aging. Previous research has documented increased risks of mortality, breast, brain, and lung cancer, mental health disorders, and an overall larger health-related burden on these individuals compared to adults without a history of craniofacial anomalies (Bille et al., 2005; Christensen, Juel, Herskind, & Murray, 2004; Christensen & Mortensen, 2002; Wehby & Cassell, 2010). Many of these individuals also mature into adults with lower self-esteem than individuals with normal anatomy (Sarwer et al., 1999). Horner et al. (1989) documented the presence of larger fat deposits around the velum and throughout pharyngeal space in individuals with normal anatomy with excessive body fat levels (participants weighed 107-153% more than ideal body weight) compared to previous reports of minimal deposits in this region in individuals of healthy weights. Findings of Mortimore, Marshall, Wraith, Sellar, and Douglas (1998) provide additional insight, as the investigators observed increased body fat deposits in the neck in non-obese and obese participants diagnosed with sleep apnea/hypopnea syndrome compared to non-obese participants without similar breathing difficulties. The investigators suggested the impact of excessive body fat in and around the neck and pharynx on respiratory integrity based on observations of increased fat deposits in these areas in non-obese participants with respiratory difficulties compared to non-obese participants with good respiratory functioning (Mortimore et al., 1998). It is possible that increased deposits of adipose tissue in and around the velum in participants in the present study may have influenced measures of soft tissue structures in the region. It is unclear what effect obesity has on measures of the pharyngeal region.

Conclusions

An overview of findings of structural and functional differences between participants with repaired cleft palate and those with normal anatomy is provided in Table 16. Findings from the present study suggest adults with repaired cleft palate demonstrated increased variability between participants and inconsistent VP function within each participant compared to the normal anatomy group. Adults with repaired cleft palate exhibited more variability in velar appearance and less precision/coordination in velar movements compared to adults with normal anatomy. Differences, however, were largely qualitative and further investigations are warranted using larger sample sizes and methods that account for the complex 3D nature of the system. The limited number of participants and high degree of variability within each group likely affected the statistical model and may have masked differences between groups that might be observed if the sample size were increased. Findings of this investigation suggest the use of structures and muscles involved in VP function for speech may vary between repaired cleft and normal anatomy. The findings and implications of these studies support the need for more research aimed at understanding which dynamic features attribute to perceptual differences noted among some speakers with repaired cleft palate. It is not known how anatomical differences, such as decreased hard palate height and length or decreased velar length impact the precision and timing of speech among cleft palate speakers. MRI is a useful tool that can combine dynamic imaging, muscle visualization, and acoustic correlates simultaneously. Future studies are needed to explore the interaction of these parameters using advanced static and dynamic protocols.

REFERENCES

Akgüner, M. (1999) Velopharyngeal anthropometric analysis with MRI in normal subjects. *Annals of Plastic Surgery,43*(2), 142-147. Retrieved from http://journals.lww.com/annalsplasticsurgery/

Akgüner, M., Karaca, C., Barutçu, A., Özaksoy, D., Yurt, A., & Vayvada, H. (1998). Evaluation of velopharyngeal pathophysiology and velopharyngeal insufficiency with magnetic resonance imaging. *European Journal of Plastic Surgery, 21,* 118-128. Retrieved from http://www.springer.com/medicine/surgery/journal/238

Atik, B., Bekerecioglu, M., Tan, O., Etik, O., Davran, R., & Arslan, H. (2008). Evaluation of dynamic magnetic resonance imaging in assessing velopharyngeal insufficiency during phonation. *The Journal of Craniofacial Surgery, 19*(3), 566-572. doi: 10.1097/SCS. 0b013e31816ae746

Bae, Y., Kuehn, D. P., Conway, C. A., & Sutton, B. P. (2011a) Real-time magnetic resonance imaging of velopharyngeal activity with simultaneous speech recordings. *Cleft Palate-Craniofacial Journal, 48*(6), 695-707. doi: 10.1597/09-158

Bae, Y., Kuehn, D.P., Sutton, B.P., Conway, C.A., & Perry, J.L. (2011b). Three-dimensional magnetic resonance imaging of velopharyngeal structures. *Journal of Speech, Language, and Hearing Research, 54,* 1538-1545. doi: 10.1044/1092-4388(2011/10-0021)

Bell-Berti, F. (1976). An electromyographic study of velopharyngeal function in speech. *Journal of Speech and Hearing Research, 19,* 225-240. Retrieved from http://jslhr.asha.org/

Bell-Berti, F., & Krakow, R. A. (1990). Anticipatory velar lowering: A coproduction account. *Haskins Laboratories Status Report on Speech Research*, SR-103/104, 21-38.

Bille, C., Winther, J. F., Bautz, A., Murray, J. C., Olsen, J., & Christensen, K. (2005). Cancer

risks in persons with oral cleft—A population-based study of 8,093 cases. *American Journal of Epidemiology, 161*(11), 1047-1055. doi: 10.1093/aje/kwi132

Bishara, S. E., Krause, C. J., Olin, W. H., Weston, D., Van Ness, J., & Felling, C. (1976). Facial and dental relationships of individuals with unoperated clefts of the lip and/or palate. *Cleft Palate Journal, 8*(13), 238-252. Retrieved from http://www.cpcjournal.org/

Boersma, P., & Weenick, D. (2013). Praat: Doing phonetics by computer (Version 5.3.53). [Computer program]. Retrieved from http://www.praat.org/

Bzoch, K. R. (1968). Variations in velopharyngeal valving: The factor of vowel changes. *Cleft Palate Journal, 5*, 211-218. Retrieved from http://www.cpcj.org/

Christensen, K., & Mortensen, P. B. (2002). Facial clefting and psychiatric diseases: A follow-up of the Danish 1936-1987 facial cleft cohort. *Cleft Palate-Craniofacial Journal, 39*(4), 392-396. Retrieved from http://www.cpcj.org/

Christensen, K., Juel, K., Herskind, A. M., & Murray, J. C. (2004). Long term follow up study of survival associated with cleft lip and palate at birth. *British Medical Journal, 328*(1405). doi: 10.1136/bmj.38105.559120.7C

Coccaro, P. J., Subtelny, J. D., & Pruzansky, S. (1962). Growth of soft palate in cleft palate children: A serial cephalometric study. *Plastic and Reconstructive Surgery, 30*(1), 43-55. Retrieved from http://journals.lww.com/plasreconsurg/pages/default.aspx

Crabb, J. J., & Foster, T. D. (1977). Growth defects in unrepaired unilateral cleft lip and palate. *Oral Surgery, 44*(3), 329-335. Retrieved from http://onlinelibrary.wiley.com/journal/10.1111/%28ISSN%291752-248X

Croft, C. B., Shprintzen, R. J., & Rakoff, S. J. (1981). Patterns of velopharyngeal valving in normal and cleft palate subjects: A multi-view videofluoroscopic and nasendoscopic

study. *The Laryngoscope, 91*, 265-271. Retrieved from http://onlinelibrary.wiley.com/journal/10.1002/(ISSN)1531-4995

Dickson, D. R. (1972). Normal and cleft palate anatomy. *Cleft Palate Journal, 9,* 280-293. Retrieved from http://www.cpcj.org/

Dickson, D. R., & Dickson, W. M. (1972). Velopharyngeal anatomy. *Journal of Speech and Hearing Research, 15,* 372-381. Retrieved from http://jslhr.asha.org/

Drissi, C., Mitrofanoff, M., Talandier, C., Falip, C., Le Couls, V., & Adamsbaum, C. (2011). Feasibility of dynamic MRI for evaluating velopharyngeal insufficiency in children. *European Journal of Radiology, 21,* 1462-1469. doi: 10.1007/s00330-011-2069-7

Ettema, S. L., & Kuehn, D. P. (1994). A quantitative histologic study of the normal human adult soft palate. *Journal of Speech and Hearing Research, 37*, 303-313. Retrieved from http://jslhr.asha.org/

Ettema, S.L., Kuehn, D.P., Perlman, A.L., & Alperin, N. (2002). Magnetic resonance imaging of the levator veli palatini muscle during speech. *Cleft Palate-Craniofacial Journal, 39*(2), 130-144. Retrieved from http://www.cpcjournal.org/

Fára, M., & Dvorák, J. (1970). Abnormal anatomy of the muscles of palatopharyngeal closure in cleft palates: Anatomical and surgical considerations based on the autopsies of 18 unoperated cleft palates. *Plastic and Reconstructive Surgery, 46*(5), 488-497. Retrieved from http://journals.lww.com/plasreconsurg/

Graber, T. M., Bzoch, K. R., & Aoba, T. (1959). A functional study of the palatal and pharyngeal structures. *The Angle Orthodontist, 29*(1), 30-40. Retrieved from http://www.angle.org/loi/angl

Ha, S., Kuehn, D.P., Cohen, M., & Alperin, N. (2007). Magnetic resonance imaging of the

levator veli palatini muscle in speakers with repaired cleft palate. *Cleft Palate-Craniofacial Journal, 44*(5), 494-505. doi: 10.1597/06-220.1

Hagerty, R. F., Hill, M. J., Pettit, H. S., & Kane, J. J. (1958). Soft palate movement in normals. *Journal of Speech and Hearing Research, 1*(4), 325-330. Retrieved from http://jslhr.asha.org/

Hoenig, J. F., & Schoener, W. F. (1992). Radiological survey of the cervical spine in cleft lip and palate. *Dentomaxillofacial Radiology, 21*, 36-39. Retrieved from http://www.birpublications.org/toc/dmfr/current

Hoopes, J. E., Dellon, A. L., Fabrikant, J. I., Edgerton, M. T., & Soliman, A. H. (1969a). Cineradiographic definition of the functional anatomy and pathophysiology of the velopharynx. *Cleft Palate Journal, 7*, 443-454. Retrieved from http://www.cpcjournal.org/

Hoopes, J. E., Dellon, A. L., Fabrikant, J. I., & Soliman, A. H. (1969b). The locus of levator veli palatini function as a measure of velopharyngeal incompetence. *Plastic and Reconstructive Surgery, 44*(2), 155-160. Retrieved from http://journals.lww.com/plasreconsurg/

Horner, R. L., Mohiaddin, R. H., Lowell, D. G., Shea, S. A., Burman, E. D., Longmore, D. B., & Guz, A. (1989). Sites and sizes of fat deposits around the pharynx in obese patients with obstructive sleep apnoea and weight matched controls. *European Respiratory Journal, 2*, 613-622. Retrieved from http://erj.ersjournals.com/

Horswell, B. B. (1991). The incidence and relationship of cervical spine anomalies in patients with cleft lip and/or palate. *Journal of Oral and Maxillofacial Surgery, 49*, 693-697. Retrieved from http://www.joms.org/

Huang, M. H., Lee, S. T., & Rajendran, K. (1998). Anatomic basis of cleft palate and velopharyngeal surgery: Implications from a fresh cadaveric study. *Journal of Plastic and Reconstructive Surgery, 101*(3), 613-627. Retrieved from http://journals.lww.com/plasreconsurg/pages/default.aspx

Ishikawa, H., Nakamura, S., Misaki, K., Kudoh, M., Fukuda, H., & Yoshida, S. (1998). Scar tissue distribution on palates and its relation to maxillary dental arch form. *Cleft Palate-Craniofacial Journal, 35*(4), 313-319. Retrieved from http://www.cpcjournal.org/

Kane, A. A., Butman, J. A., Mullick, R., Skopec, M., & Choyke, P. (2002). A new method for the study of velopharyngeal function using gated magnetic resonance imaging. *Plastic and Reconstructive Surgery, 109*(2), 472-481. Retrieved from http://journals.lww.com/plasreconsurg/

Khanna, R., Tikku, T., & Wadhwa, J. (2012). Nasomaxillary complex in size, position and orientation in surgically treated and untreated individuals with cleft lip and palate: A cephalometric overview. *Indian Journal of Plastic Surgery, 45*(1), 68-75. doi: 10.4103/0970-0358.96590

Kuehn, D. P. (1976). A cineradiographic investigation of velar movement variables in two normals. *Cleft Palate Journal*, *13*, 88-103. Retrieved from http://www.cpcjournal.org/

Kuehn, D. P., & Azzam, N. A. (1978). Anatomical characteristics of palatoglossus and the anterior faucial pillar. *Cleft Palate Journal, 15*(4), 349-359. Retrieved from http://www.cpcjournal.org/

Kuehn, D. P., Ettema, S. L., Goldwasser, M. S., & Barkmeier, J. C. (2004). Magnetic resonance imaging of the levator veli palatini muscle before and after primary palatoplasty.

Cleft Palate-Craniofacial Journal, 41(6), 584-592. Retrieved from http://www.cpcjournal.org/

Kuehn, D. P., Ettema, S. L., Goldwasser, M. S., Barkmeier, J. C., & Wachtel, J. M. (2001). Magnetic resonance imaging in the evaluation of occult submucous cleft palate. *Cleft Palate-Craniofacial Journal, 38*(5), 421-431. Retrieved from http://www.cpcjournal.org/

Kuehn, D. P., Folkins, J. W., & Cutting, C. B. (1982). Relationships between muscle activity and velar position. *Cleft Palate Journal, 19*(1), 25-35. Retrieved from http://www.cpcjournal.org/

Kuehn, D. P., & Moon, J. B. (1998). Velopharyngeal closure force and levator veli palatini activation levels in varying phonetic contexts. *Journal of Speech, Language, and Hearing Research, 41*, 51-62. Retrieved from http://jslhr.asha.org/

Kuehn, D. P., & Moon, J. B. (2005). Histologic study of intravelar structures in normal human adult specimens. *Cleft Palate-Craniofacial Journal, 42*(5), 481-489. Retrieved from http://www.cpcjournal.org/

Law, F. E., & Fulton, J. T. (1959). Unoperated oral clefts at maturation. *American Journal of Public Health and the Nation's Health, 49*(11), 1517-1524. Retrieved from http://ajph.aphapublications.org/

Lindman, R., Paulin, G., & Stal, P. S. (2001). Morphological characterization of the levator veli palatini muscle in children born with cleft palates. *Cleft Palate-Craniofacial Journal, 38*(5), 438-448. Retrieved from http://www.cpcj.org/

Lipira, A. B., Grames, L. M., Molter, D., Govier, D., Kane, A. A., & Woo, A. S. (2011). Videofluoroscopic and nasendoscopic correlates of speech in velopharyngeal dysfunction. *Cleft Palate-Craniofacial Journal, 48*(5), 550-560. doi: 10.1597/09-203

Liss, J. M. (1990). Muscle spindles in the human levator veli palatini and palatoglossus muscles. *Journal of Speech and Hearing Research, 33*, 736-746. Retrieved from http://jslhr.asha.org/

Maturo, S., Silver, A., Nimkin, K., Sagar, P., Ashland, J., van der Kouwe, A. J., & Hartnick, C. (2012). MRI with synchronized audio to evaluate velopharyngeal insufficiency. *Cleft Palate-Craniofacial Journal, 49*(6), 761-763. doi: 10.1597/10-255

McKerns, D., & Bzoch, K. R. (1970). Variations in velopharyngeal valving: The factor of sex. *Cleft Palate Journal, 7*, 652-662. Retrieved from http://www.cpcj.org/

McGowan, J. C., Hatabu, H., Yousem, D. M., Randall, P., & Kressel, H. Y. (1992). Evaluation of soft palate function with MRI: Application to the cleft palate patient. *Journal of Computer Assisted Tomography, 16*(6), 877-882. Retrieved from http://journals.lww.com/jcat/

Mehendale, F. V. (2004). Surgical anatomy of the levator veli palatini: A previously undescribed tendinous insertion of the anterolateral fibers. *Plastic and Reconstructive Surgery, 114*(2), 307-315. doi: 10.1097/01.PRS.0000131869.45025.5A

Moll, K. L. (1962). Velopharyngeal closure on vowels. *Journal of Speech and Hearing Research, 5*, 30-37. Retrieved from http://jslhr.asha.org/

Moon, J. B., Kuehn, D. P., & Huisman, J. J. (1994a). Measurement of velopharyngeal closure force during vowel production. *Cleft Palate-Craniofacial Journal, 31*(5), 356-363. Retrieved from http://www.cpcjournal.org/

Moon, J. B., Smith, A. E., Folkins, J. W., Lemke, J. H., & Gartlan, M. (1994b). Coordination of velopharyngeal muscle activity during positioning of the soft palate. *Cleft Palate-Craniofacial Journal, 31*(1), 356-363. Retrieved from http://www.cpcjournal.org/

Mortimore, I. L., Marshall, I., Wraith, P. K., Sellar, R. J., & Douglas, N. J. (1998). Neck and total body fat deposition in nonobese and obese patients with sleep apnea compared with that in control subjects. *American Journal of Respiratory and Critical Care Medicine, 157*(1), 280-283. Retrieved from http:// http://www.atsjournals.org/journal/ajrccm

NessAiver, M. S., Stone, M., Parthasarathy, V., Kahana, Y., & Paritsky, A. (2006). Recording high quality speech during tagged cine-MRI studies using a fiber optic microphone. *Journal of Magnetic Resonance Imaging, 23*, 92-97. doi: 10.1002/jmri.20463

Özgür, F., Tunçbilek, G., & Cila, A. (2000). Evaluation of velopharyngeal insufficiency with magnetic resonance imaging and nasoendoscopy. *Annals of Plastic Surgery, 44*(1), 8-13. Retrieved from http://journals.lww.com/annalsplasticsurgery/

Perry, J. L. (2011). Variations in velopharyngeal structures between upright and supine positions using upright magnetic resonance imaging. *Cleft Palate-Craniofacial Journal, 48*(2), 123-133. doi: 10.1597/09-256

Perry, J. L., & Kuehn, D. P. (2007). Three-dimensional computer reconstruction of the levator veli palatini muscle in Situ using magnetic resonance imaging. *Cleft Palate-Craniofacial Journal, 44*(4), 421-423. doi: 10.1597/06-137.1

Perry, J. L., & Kuehn, D. P. (2009). Magnetic resonance imaging and computer reconstruction of the velopharyngeal mechanism. *The Journal of Craniofacial Surgery, 20*(2), 1739-1746. doi: 10.1097/SCS.0b013e3181b5cf46

Perry, J.L., Kuehn, D.P., & Sutton, B.P. (2013). Morphology of the levator veli palatini muscle using magnetic resonance imaging. *Cleft Palate-Craniofacial Journal, 50(*1), 64-75. doi: 10.1597/11-125

Perry, J. L., Sutton, B. P., Kuehn, D. P., & Gamage, J. K. (2014). Using MRI for assessing

velopharyngeal structures and function. *Cleft Palate-Craniofacial Journal, 51*(4), 476-485. doi: 10.1597/12-083

Perry, J. L., Kuehn, D. P., Sutton, B. P., Gamage, J. K., & Fang, X. (in press). Anthropometric analysis of the velopharynx and related craniometric dimensions in three adult populations using MRI. *Cleft Palate-Craniofacial Journal*. doi: 10.1597/14-015

Perry, J. L., Kuehn, D. P., Sutton, B. P., Goldwasser, M. S., & Jerez, A. D. (2011). Craniometric and velopharyngeal assessment of infants with and without cleft palate. *The Journal of Craniofacial Surgery, 22*(2), 499-503. doi: 10.1097/SCS.0b013e3182087378

Pigott, R. W. (1969). The nasendoscopic appearance of the normal palato-pharyngeal valve. *Plastic and Reconstructive Surgery, 43*(1), 19-24. Retrieved from http://journals.lww.com/plasreconsurg/

Reichert, H. (1970). Osteoplasty in complete clefts of the secondary palate. *British Journal of Plastic Surgery, 23*(1), 45-49. Retrieved from http://www.jprasurg.com/

Rowe, M. R., & D'Antonio, L. L. (2005). Velopharyngeal dysfunction: Evolving developments in evaluation. *Current Opinion in Otolaryngology & Head and Neck Surgery, 13*(6), 366-370. Retrieved from http://journals.lww.com/co-otolaryngology/

Sandham, A. (1986). Cervical vertebral anomalies in cleft lip and palate. *Cleft Palate Journal, 23,* 206-214. Retrieved from http://www.cpcjournal.org/

Sandham, A., & Cheng, L. (1988). Cranial base and cleft lip and palate. *The Angle Orthodontist,* 163-168. Retrieved from http://www.angle.org/loi/angl

Sarwer, D. B., Bartlett, S. P., Whitaker, L. A., Paige, K. T., Pertschuk, M. J., & Wadden, T. A.

(1999). Adult psychological functioning of individuals born with craniofacial anomalies. *Plastic and Reconstructive Surgery, 103*(2), 412-418. Retrieved from http://journals.lww.com/plasreconsurg/

Satoh, K., Wada, T., Tachimura, T., Sakoda, S., & Shiba, R. (1999). A cephalometric study of the relationship between the level of velopharyngeal closure and the palatal plane in patients with repaired cleft palate and controls without clefts. *British Journal of Oral and Maxillofacial Surgery, 37,* 486-489. Retrieved from http://www.bjoms.com/

Satoh, K., Wada T., Tachimura, T., & Shiba, R. (2002). The effect of growth of nasopharyngeal structures in velopharyngeal closure in patients with repaired cleft palate and controls without clefts: A cephalometric study. *British Journal of Oral and Maxillofacial Surgery, 40*(2), 105-109. doi: 10.1054/bjom.2001.0749

Scott, A. D., Wylezinska, M., Birch, M. J., & Miquel, M. E. (2014). Speech MRI: Morphology and function. *Physica Medica, 30*, 604-618. doi: 10.1016/j.ejmp.2014.05.001

Seaver, E. J., & Kuehn, D. P. (1980). A cineradiographic and electromyographic investigation of velar positioning in non-nasal speech. *Cleft Palate Journal*, 17(3), 216-226. Retrieved from http://www.cpcj.org/

Shibaski, Y., & Ross, R. B. (1969). Facial growth in children with isolated cleft palate. *Cleft Palate Journal, 6,* 290-302. Retrieved from http://www.cpcjournal.org/

Shimokawa, T., Yi, S., & Tanaka, S. (2005). Nerve supply to the soft palate muscles with special reference to the distribution of the lesser palatine nerve. *Cleft Palate-Craniofacial Journal, 42*(5), 495-500. Retrieved from http://www.cpcjournal.org/

Shinagawa, H., Ono, T., Honda, E., Masaki, S., Shimada, Y., Fujimoto, I., … Ohyama, K. (2005). Dynamic analysis of articulatory movement using magnetic resonance imaging

movies: Methods and implications in cleft lip and palate. *Cleft Palate-Craniofacial Journal, 42*(3), 225-230. doi: 10.1597/03-007.1

Skolnick, M. L. (1970, April). *Videofluoroscopic examination of the velopharyngeal portal during phonation in lateral and base projections—A new technique for studying the mechanics of closure.* Paper presented at the 28th Annual Meeting of the American Cleft Palate Association, Portland, Oregon.

Skolnick, M. L., McCall, G. N., & Barnes, M. (1972, April). *The sphincteric mechanism of velopharyngeal closure.* Paper presented at the 30th Annual Meeting of the American Cleft Palate Association, Phoenix, Arizona.

Subtelny, J. D. (1957). A cephalometric study of the growth of the soft palate. *Plastic and Reconstructive Surgery, 19*(1), 49-62. Retrieved from http://journals.lww.com/plasreconsurg/

Sutton, B. P., Conway, C. A., Bae, Y., Brinegar, C., Liang, Z. P., & Kuehn, D. P. (2009, September). *Dynamic imaging of speech and swallowing with MRI*. Paper presented at the 31st Annual International Conference of the IEEE Engineering in Medical & Biology Society, Minneapolis, Minnesota.

Sutton, B. P., Conway, C. A., Bae, Y., Seethamraju, R., & Kuehn, D. P. (2010). Faster dynamic imaging of speech with field inhomogeneity correlated spiral fast low angle shot (FLASH) at 3T. *Journal of Magnetic Resonance Imaging, 32,* 1228-1237. doi: 10.1002/ jmri.22369

Tian, W., & Redett, R. J. (2009). New velopharyngeal measurements at rest and during speech: Implications and applications. *Journal of Craniofacial Surgery, 20*(2), 532-539. doi: 10.1097/SCS.0b013e31819b9fbe

Tian, W., Li, Y., Yin, H., Zhao, S., Li, S., Wang, Y., & Shi, B. (2010a). Magnetic resonance imaging assessment of velopharyngeal motion in Chinese children after primary palatal repair. *The Journal of Craniofacial Surgery, 21*(2), 578-587. doi: 10.1097/SCS.0b013e3181d08bd1

Tian, W., Yin, H., Reddett, R. J., Shi, B., Shi, J., Zhang, R., & Zheng, Q. (2010b). Magnetic resonance imaging assessment of the velopharyngeal mechanism at rest and during speech in Chinese adults and children. *Journal of Speech, Language, and Hearing Research, 53,* 1595-1615. doi: 10.1044/1092-4388(2010/09-0105)

Tian, W., Yin, H., Li, Y., Zhao, S., Zheng, Q., & Shi, B. (2010c). Magnetic resonance imaging of velopharyngeal structures in Chinese children after primary palatal repair. *The Journal of Craniofacial Surgery, 21*(2), 568-577. doi: 10.1097/SCS.0b013e3181d08bd1

Uğar, D. A., & Semb, G. (2001). The prevalence of anomalies of the upper cervical vertebrae in subjects with cleft lip, cleft palate, or both. *Cleft Palate-Craniofacial Journal, 38*(5), 498-503. Retrieved from http://www.cpcjournal.org/

Wada, T., Satoh, K., Tachimura, T., & Tatsuta, U. (1997). Comparison of nasopharyngeal growth between patients with clefts and noncleft controls. *Cleft Palate-Craniofacial Journal, 34*(5), 405-409. doi: 10.1597/1545-1569

Wada, T., & Miyazaki, T. (1975). Growth and changes in maxillary arch form in complete unilateral cleft lip and cleft palate children. *Cleft Palate Journal, 12*, 115-130. Retrieved from http://www.cpcjournal.org/

Warren, D. W., Dalston, R. M., & Mayo, R. (1993). Hypernasality in the presence of "adequate" velopharyngeal closure. *Cleft Palate-Craniofacial Journal, 30*(2), 150-154. Retrieved from http://www.cpcjournal.org/

Wehby, G. L., & Cassell, C. H. (2010). The impact of orofacial clefts on quality of life and health care use and costs. *Oral Diseases, 16*(1), 3-10. doi: 10.1111/j.1601-0825.2009.01588.x

Witt, P. D., Marsh, J. L., McFarland, E. G., & Riski, J. E. (2000). The evolution of velopharyngeal imaging. *Annals of Plastic Surgery*, 45(6), 665-673. Retrieved from http://journals.lww.com/annalsplasticsurgery/

Yunusova, Y., Baljko, M., Pintilie, G., Rudy, K., Faloutos, P., & Daskalogiannakis, J. (2012). Acquisition of the 3D surface of the palate by in-vivo digitization with Wave. *Speech Communication, 54*, 923-931. doi: 10.1016/j.specom.2012.03.006

Zajac, D. J., Cevidanes, L., Shah, S., & Haley, K. L. (2012). Maxillary arch dimensions and spectral characteristics of children with cleft lip and palate who produce middorsum palatal stops. *Journal of Speech, Language, and Hearing Research, 55*, 1876-1886. doi: 10.1044/1092-4388(2012/11-0340)

TABLES AND FIGURES

Table 1. *Demographics of Participants with Normal Anatomy*

Participant	Gender	Age (years)	Weight (kg)	Height (cm)
S1	Female	22	56	165
S2	Male	25	65	180
S3	Female	22	58	168
S4	Male	20	83	185
S5	Female	26	74	168
S6	Male	32	61	167
Mean (SD)		24.79 (4.45)	66.15 (10.42)	172.22 (8.29)

Table 2. *Demographics of Participants with Repaired Cleft Palate*

Participant	Gender	Age (years)	Weight (kg)	Height (cm)	Cleft Type
C1	Female	24	81	165.1	BCLP
C2	Male	22	106	185.42	BCLP
C3	Female	36	64	167.64	BCLP
C4	Male	32	127	182.88	BCL & Primary Palate
C5	Male	20	45	175.26	CP Only
C6	Female	19	95	165.1	CP Only
Mean (SD)		25.83 (6.98)	86.33 (29.5)	173.57 (9.04)	

Note. BCLP = bilateral cleft lip and palate; BCL = bilateral cleft lip; CP Only = isolated cleft palate

Table 3. *Magnetic Resonance Imaging Protocol*

	Static 3D MRI Parameters	**Dynamic MRI Parameters**
Resolution	.8mm isotropic	1.875 x 1.875 x 8 mm^3
Field of view	256 x 192 x 153.6 mm^3	240 x 240 x 8 mm^3
Pulse sequence	SPACE: T2 Turbo Spin Echo. Variable flip angle	FLASH: GRE six-shot spiral
Repetition time	2,500 ms	9 ms
Echo time	268 ms Echo train length: 171	Alternating between 1.3 and 1.8 ms
Length of scan	4 minutes and 52 seconds for 1 static volume	50.5 seconds for 799 native frame rate images or 1515 sliding window images at 30 fps

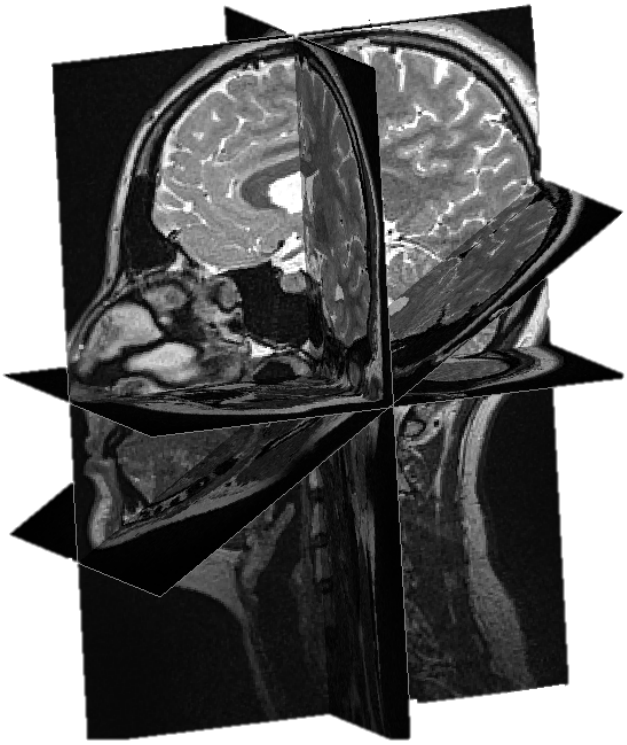

Figure 1. Representation of midsagittal, axial, coronal, and oblique coronal image planes obtained using 3D MRI.

Table 4. *Descriptions of Static Cranial Measures*

Parameter	Description
Nasion—sella turcica	Distance between the nasion and sella turcica
Basion—sella turcica	Distance between the basion and sella turcica
Opithsion—basion	Distance between the opithsion and basion
NSB angle	Anterior cranial base angle formed at intersection of Nasion-Sella turcica and Basion-Sella turcica
SBO angle	Posterior cranial base angle formed at the junction of Basion-Sella turcica and Opithsion-Basion
ANS to basion	Distance between the anterior border of the hard palate measured posteriorly to the basion
Facial height	Length of the anterior portion of the face measured as nasion to menton
Cranial length	Length of greatest anterior to posterior distance across the cranium
Cranial width	Length of greatest horizontal distance across the cranium
Index	**Description**
Cranial index	(cranial length) / (cranial width)
Cranial base index	(ANS to basion) / (levator origin to origin distance)

Table 5. *Descriptions of Static Velopharyngeal Measures*

Parameter	Description
Palate length	Palate length measured as the distance between the anterior and posterior borders of the hard palate
PNS to incisive foramen	Distance between posterior border of the hard palate and the canal for the incisive foramen
Palate width	Distance between the free lingual gingival margin of the first molar on each side
Palate height	Height of the palate measured perpendicular to the palatal width line extending to the roof of the hard palate in the region of the palatal vault
Pharyngeal depth	Distance from the posterior border of the hard palate measured posteriorly to the posterior pharyngeal wall along the hard palate plane
PNS to levator insertion	Functional portion of the velum measured as the distance between the posterior border of the hard palate and point of levator muscle insertion into the velum
Velar knee – PPW	Distance between the velar knee and the posterior pharyngeal wall
Velar length	Linear measure between the posterior border of the hard palate and inferior tip of uvula
Velar thickness	Distance between oral surface of velum and velar knee
Index	**Description**
Velopharyngeal (VP) ratio	(velar length) / (pharyngeal depth)

Figure 2. Midsagittal view of MR image displaying points of interest. N = nasion; S = sella turcica; B = basion; O = opithsion; ANS = anterior border of the hard palate; IF = canal for incisive foramen; PNS = posterior border of the hard palate; K = velar knee; U = inferior tip of the velum (uvula); PPW = posterior pharyngeal wall; M = menton.

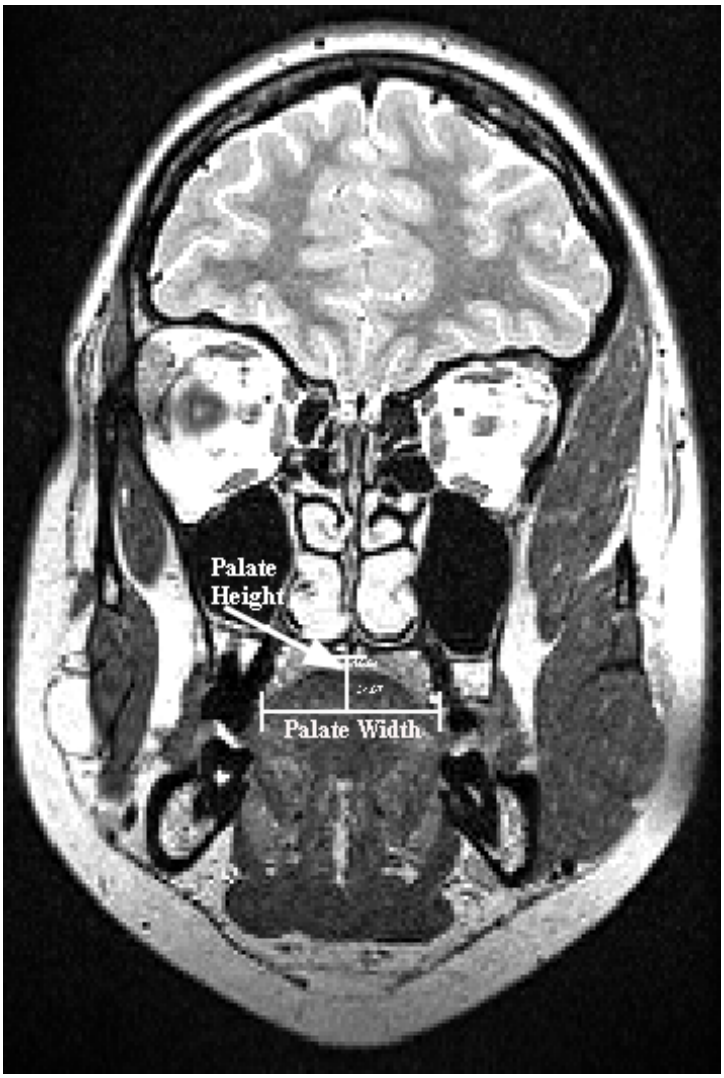

Figure 3. Coronal view of MR image displaying measures of palate width and palate height.

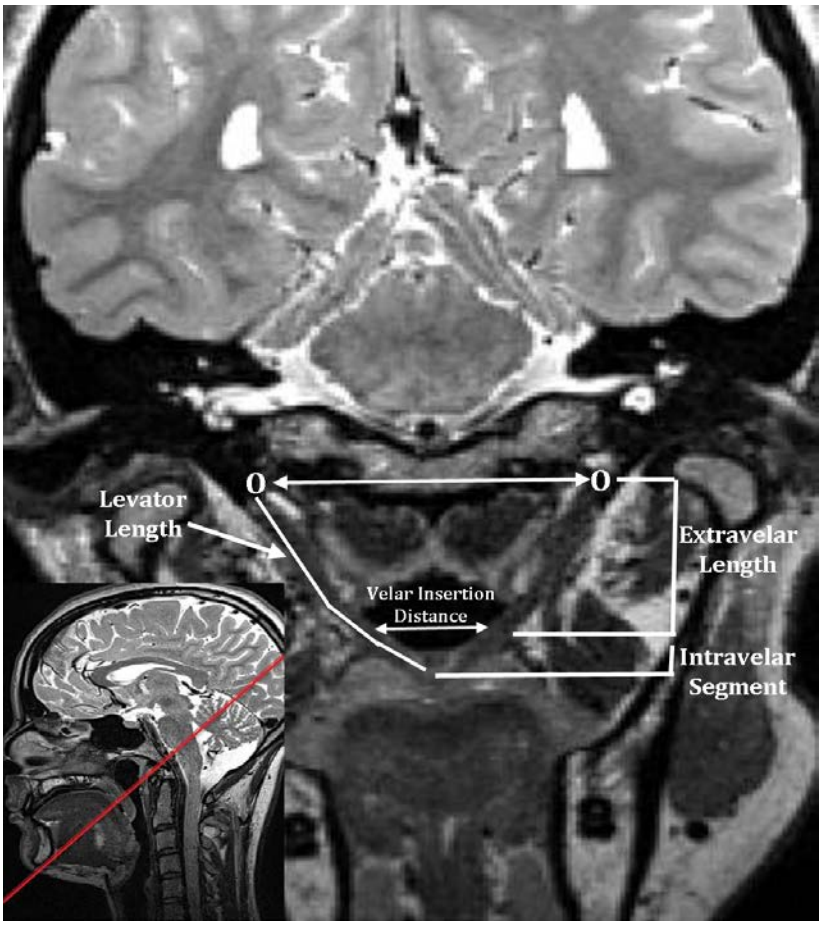

Figure 4. Oblique coronal plane of MR image displaying full sling of the levator muscle. The image in the lower left displays the sampling plane used to obtain oblique coronal plane. O = each point of origin of the levator muscle at the cranial base.

Table 6. *Descriptions of Static Levator Muscle Measures*

Parameter	Description
Distance between origin points	Distance between the right levator muscle origin at the cranial base and left levator muscle origin on the other side
Average muscle length	Average of right and left levator muscle length measures from origin at cranial base to middle of muscular sling within the velum
Average angle of origin	Average of right and left angles between origin to origin width and insertion of muscle fibers at cranial base
Average extravelar muscle length	Average of right and left levator muscle fibers from origin at either side of the cranial base to insertion of levator muscle into either side of the velum
Intravelar segment length	Length of the levator muscle within the velum
Velar insertion distance	Distance between points of levator insertion into the velum

Table 7. *Descriptions of Dynamic Velar and Levator Muscle Measures*

Velar Measures	
α angle	Angle at which soft palate travels through during velopharyngeal closure
β angle	Genu angle during velopharyngeal closure
Velar stretch	Distance between the posterior border of the hard palate and velar knee
Levator Measure	
Average muscle length	Average of right and left muscle length measurements

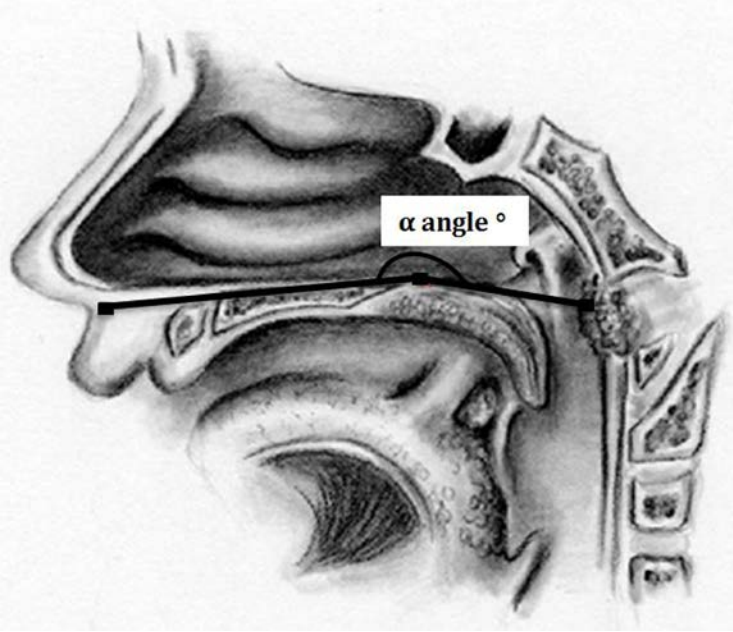

Figure 5. Visualization of α angle measure.

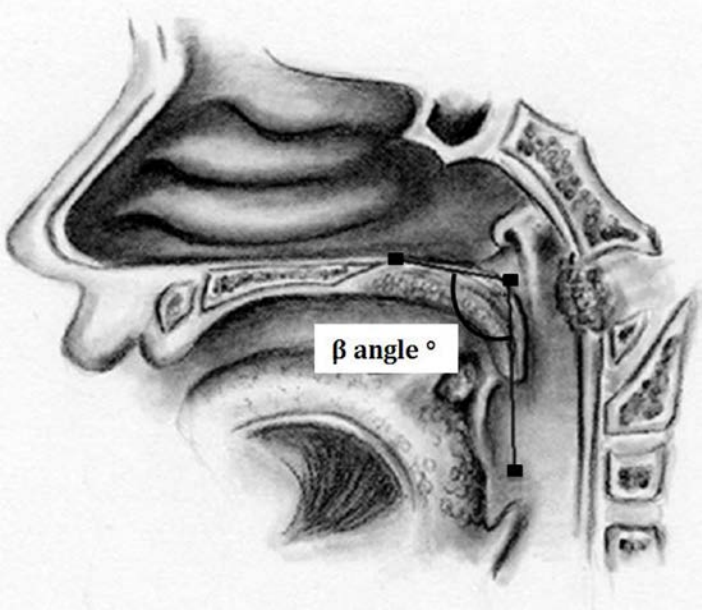

Figure 6. Visualization of β angle measure.

Table 8. *Mean (SD) Static Cranial Measures for Participants with Normal Anatomy and Participants with Repaired Cleft Palate*

Parameter	Normal Anatomy	Repaired Cleft Palate	Sig. (2-tailed)
Nasion—sella turcica	61.31 (3.92)	62.01 (4.02)	.766
Basion—sella turcica	44.32 (2.06)	45.06 (3.61)	.672
Opithsion—basion	36.04 (1.98)	38.21 (1.72)	.070
NSB angle	125.08 (6.58)	123.97 (4.17)	.733
SBO angle	140.63 (6.29)	128.58 (5.03)	.004*
ANS—basion	105.66 (3.67)	103.65 (3.81)	.376
Facial height	110.64 (6.84)	119.11 (9.92)	.116
Cranial length	191.2 (4.12)	195.06 (5.2)	.185
Cranial width	154.5 (7.5)	153.55 (8.84)	.845
Cranial index	1.24 (0.06)	1.27 (0.06)	.366
Cranial base index	1.86 (0.14)	1.88 (0.14)	.883

* $\alpha < 0.05$

Note. All measures of interest are reported in millimeters (mm) with exceptions including NSB angle (°), SBO angle (°), and index measures.

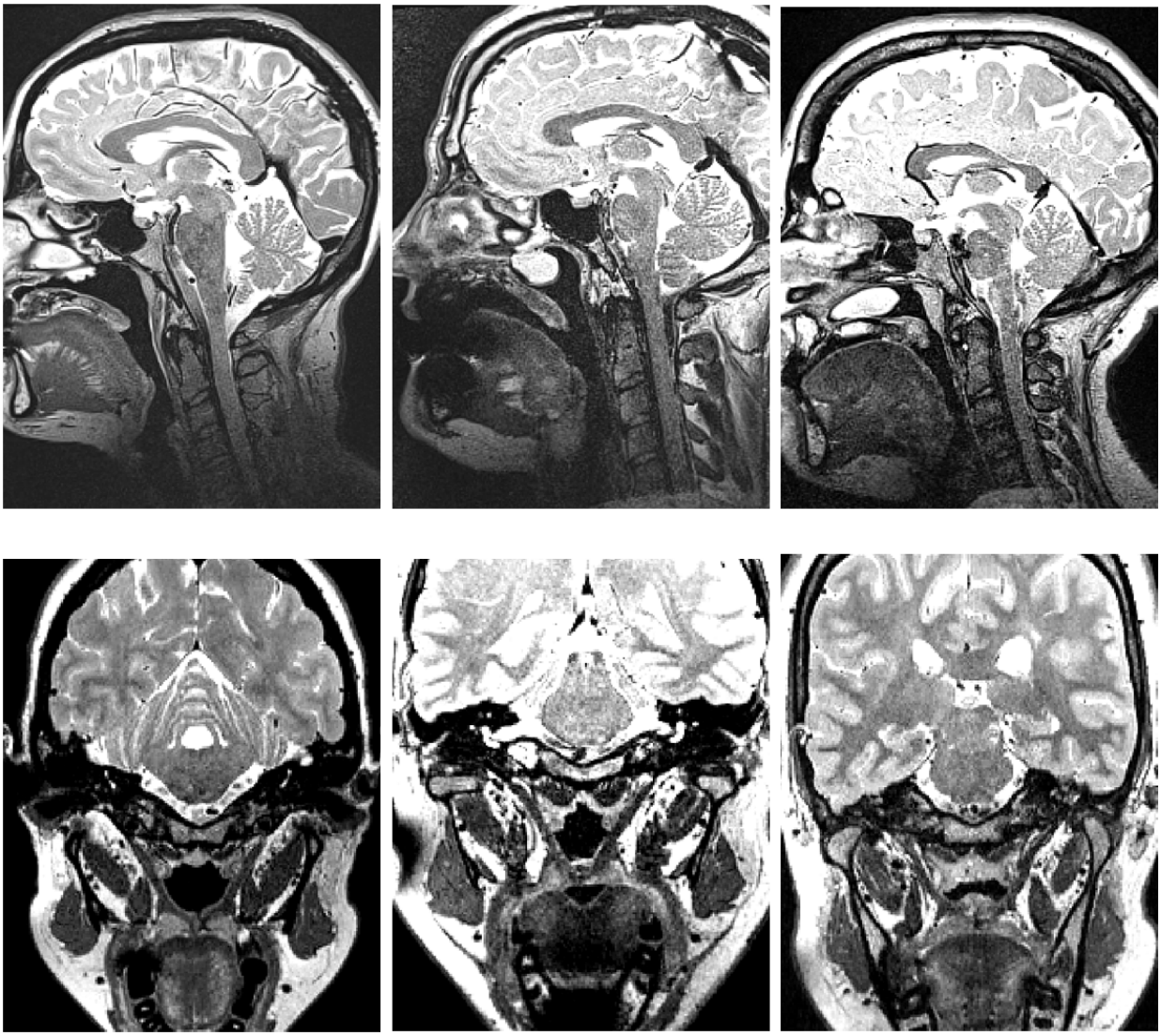

Figure 7. Midsagittal (top) and oblique coronal (bottom) image planes from selected participants with repaired cleft anatomy. In the midsagittal images (top,) note the lack of posterior extension of the hard palate in the top left, altered hard palate and velar morphology in the top middle, and unusual velar morphology in the top right. In the oblique coronal images (bottom,) note the midline separation of the levator muscle in the bottom left, V-shape configuration and visible musculus uvulae fibers in the bottom middle, and the odd bulge on the nasal surface of the levator in the bottom right.

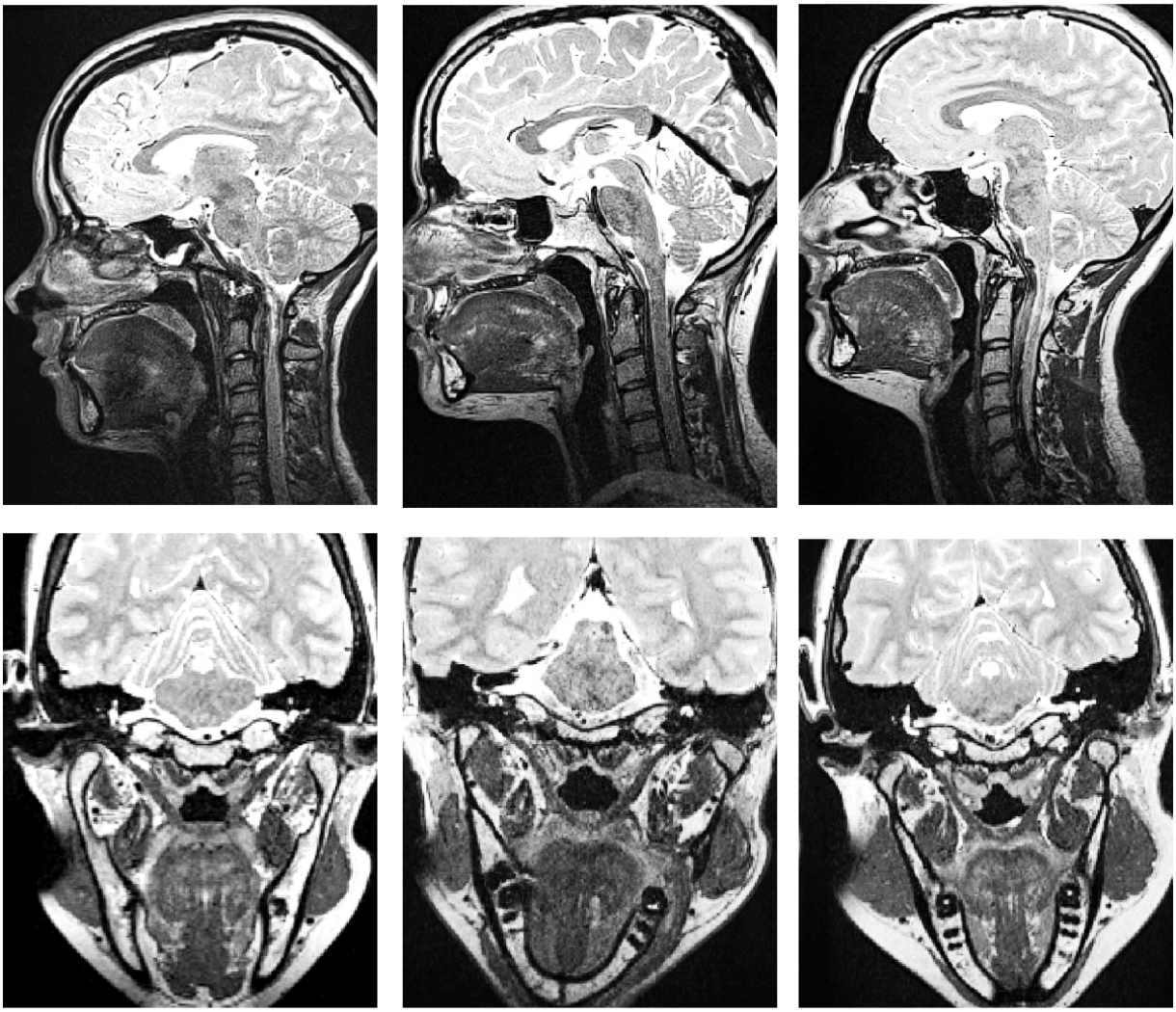

Figure 8. Midsagittal (top) and oblique coronal (bottom) image planes from selected participants with normal anatomy. Note the consistent velar and levator morphology across the three participants. Velar thickness is consistent along the entire length of the velum. Levator configuration is consistent and musculus uvulae fibers are visible in the middle of the muscular sling within the velum.

Table 9. *Mean (SD) Static Measures of Levator Muscle Morphology for Participants with Normal Anatomy and Participants with Repaired Cleft Palate*

Parameter	Normal Anatomy	Repaired Cleft Palate	Sig. (2-tailed)
Distance between origin points	56.91 (4.27)	55.47 (3.86)	.554
Average muscle length	45.29 (3.54)	44.36 (5.04)	.722
Average angle of origin	56.09 (3.27)	55.88 (5.34)	.937
Average extravelar length	31.1 (4.57)	31.3 (3.12)	.930
Intravelar segment length	31.81 (1.55)	31.03 (2.16)	.490
Velar insertion distance	26.04 (3.96)	26.01 (4.47)	.990

* $\alpha < .05$

Note. All measures of interest are reported in millimeters (mm) with exception of average angle of origin (°).

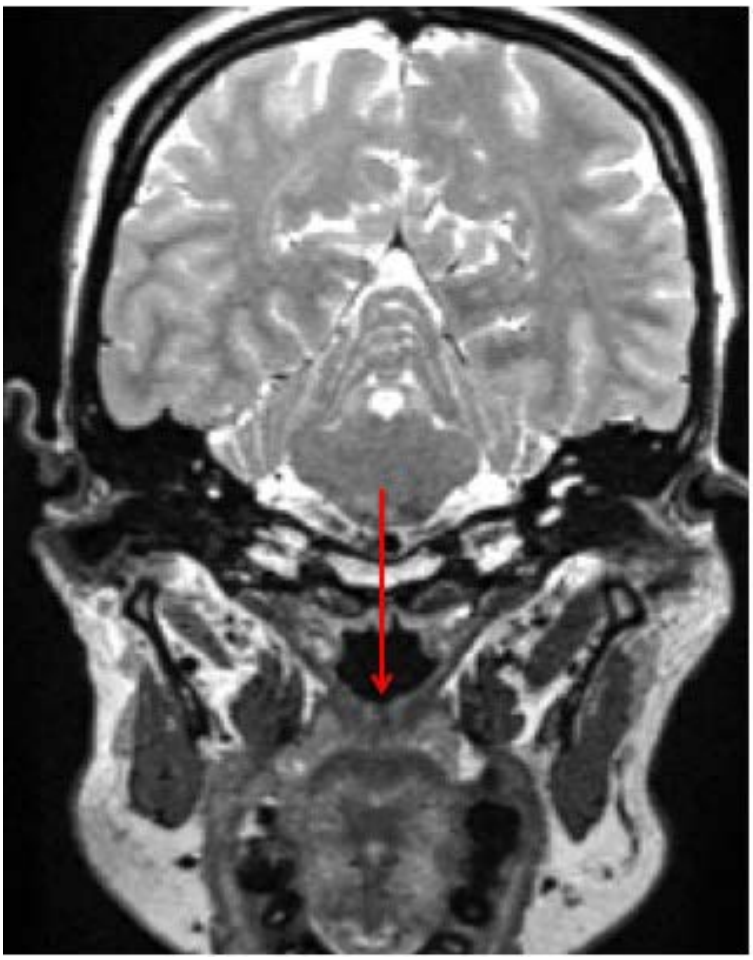

Figure 9. Oblique coronal plane from one participant with repaired cleft palate displaying possible midline separation of the levator muscle/atypically shaped fibers of the musculus uvulae, indicated by the red arrow.

Table 10. *Mean (SD) Static Velopharyngeal Measures for Participants with Normal Anatomy and Participants with Repaired Cleft Palate*

Parameter	Normal Anatomy	Repaired Cleft Palate	Sig. (2-tailed)
Palate length	56.33 (1.8)	51.73 (3.87)	.025*
PNS-incisive foramen	37.62 (1.92)	34.44 (5.22)	.192
Palate width	34.85 (3.67)	33.63 (4.63)	.623
Palate height	12.05 (2.39)	8.73 (1.41)	.015*
Pharyngeal depth	20.89 (2.52)	28.15 (3.49)	.02*
PNS—levator insertion	12.64 (2.72)	12.19 (1.86)	.746
Velar length	30.12 (4.18)	24.13 (6.27)	.08
Velar thickness	10.89 (1.87)	11.01 (1.0)	.894
Velar knee—PPW	11.53 (0.92)	11.2 (2.03)	.726
VP ratio	1.28 (0.26)	0.85 (0.18)	.008*

* $\alpha < .05$

Note. All measures of interest are reported in millimeters (mm) with exception of VP ratio.

Table 11. *Average Percent Change in Levator Muscle Length for Participants with Normal Anatomy and Participants with Repaired Cleft Palate During Production of "ampa"*

	"a"	"m"	"p"	"a"
Normal anatomy	- 1.67 %	- 1.46 %	- 20.77 %	- 16.2 %
Repaired cleft palate	- 7.32 %	+ .82 %	- 11.61 %	- 10.82%
Sig. (2-tailed)	.485	.586	.084	.420

* $\alpha < .05$

Table 12. *Mean (SD) Levator Muscle Length for Participants with Normal Anatomy and Participants with Repaired Cleft Palate During Production of Phonemes in "ampa"*

	Rest	"a"	"m"	"p"	"a"
Normal anatomy	44.06 (3.85)	39.20 (5.63)	43.45 (5.56)	34.87 (2.95)	36.93 (4.95)
Repaired cleft palate	43.53 (6.14)	40.36 (6.33)	43.97 (7.05)	38.76 (8.35)	38.94 (8.09)

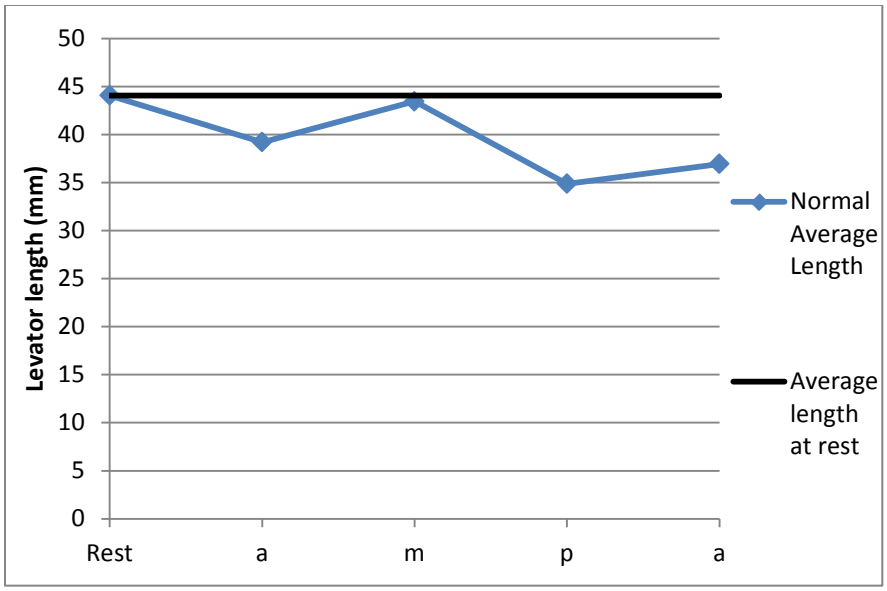

Figure 10. Graphical display of average levator muscle length changes (in millimeters) from rest to production of phonemes in "ampa" for participants with normal anatomy

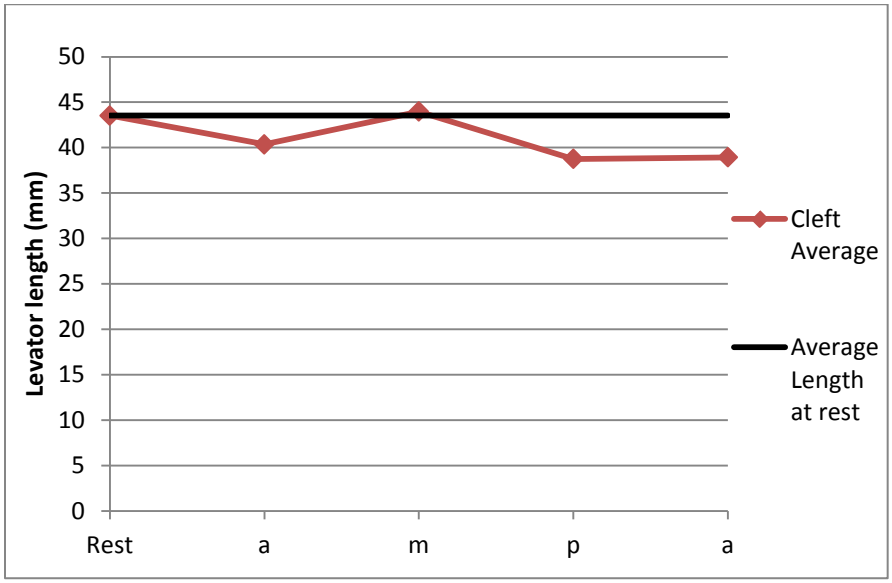

Figure 11. Graphical display of average levator muscle length changes (in millimeters) from rest to production of phonemes in "ampa" for participants with repaired cleft palate

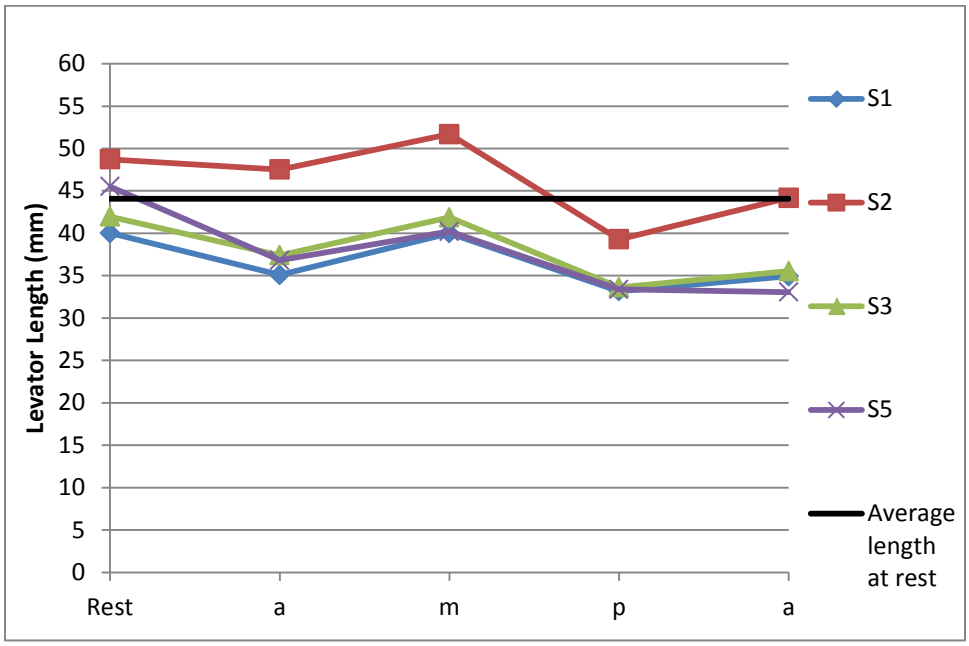

Figure 12. Graphical display of levator muscle length changes (in millimeters) from rest to production of phonemes in "ampa" for participants with normal anatomy

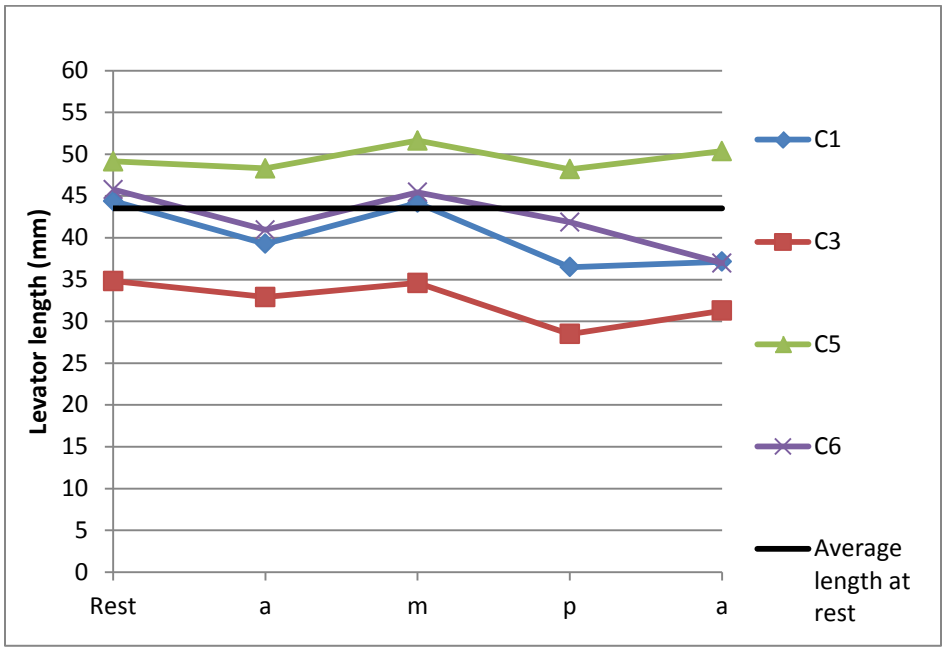

Figure 13. Graphical display of levator muscle length changes (in millimeters) from rest to production of phonemes in "ampa" for participants with repaired cleft palate

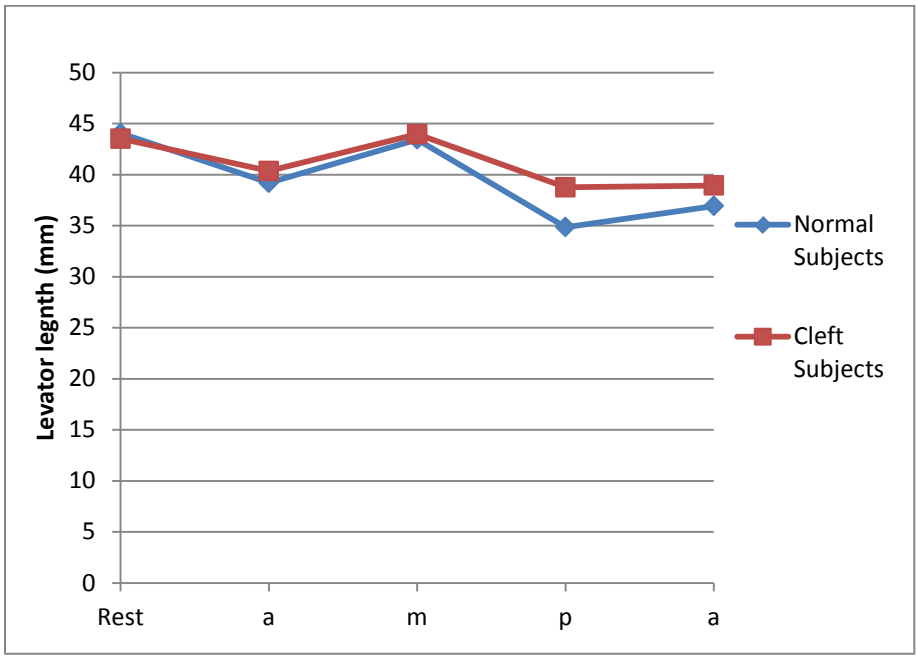

Figure 14. Graphical display of average levator muscle length changes (in millimeters) from rest to production of phonemes in "ampa" for participants with normal anatomy and participants with repaired cleft palate

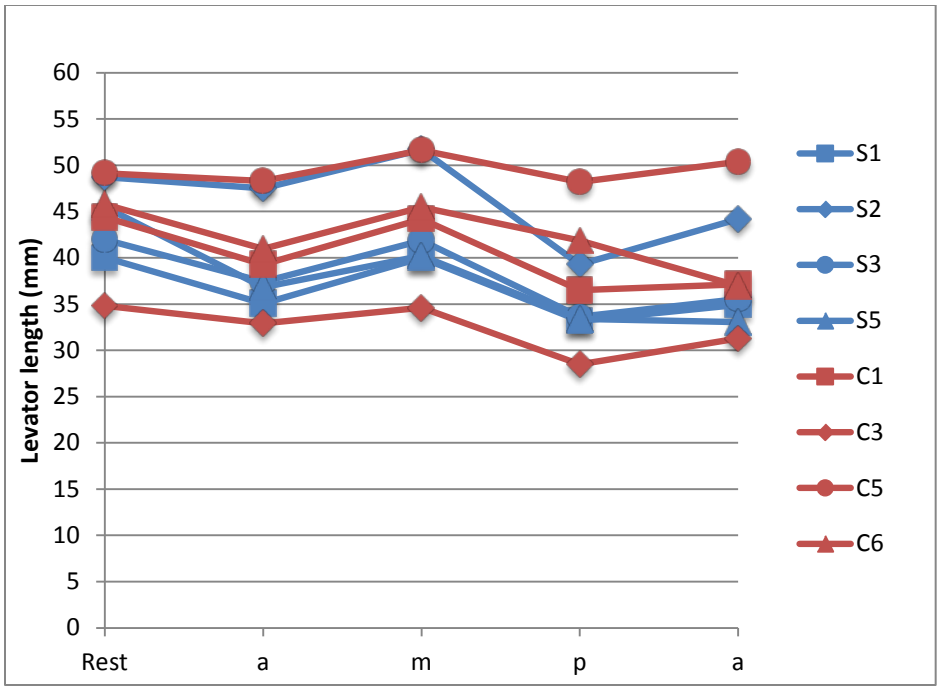

Figure 15. Graphical display of levator muscle length changes (in millimeters) from rest to production of phonemes in "ampa" for participants within each study group

Table 13. *Average Percent Change in α Angle During Production of "ampa" for Participants with Normal Anatomy and Participants with Repaired Cleft Palate*

	"a"	**"m"**	**"p"**	**"a"**
Normal anatomy	+ 0.77%	+ 5.49 %	+ 0.54 %	+ 0.46 %
Repaired cleft palate	- 4.3 %	+ 3.42 %	- 6.08 %	- 5.84 %
Sig. (2-tailed)	.007*	.673	.006*	$p < .001$*

* $\alpha < .05$

Table 14. *Average Percent Change in β Angle During Production of "ampa" for Participants with Normal Anatomy and Participants with Repaired Cleft Palate*

	"a"	**"m"**	**"p"**	**"a"**
Normal anatomy	-7.02%	+13.23%	-17.84%	-20.33%
Repaired cleft palate	-11.4%	+6.12%	-15.14%	-14.07%
Sig. (2-tailed)	.034*	.022*	.167	.045*

* $\alpha < .05$

Table 15. *Average Percent Change in Velar Stretch During Production of "ampa" for Participants with Normal Anatomy and Participants with Repaired Cleft Palate*

	"a"	**"m"**	**"p"**	**"a"**
Normal anatomy	+ 18.19 %	- 10.14 %	+ 55.55 %	+ 46.74 %
Repaired cleft palate	+ 20.2 %	- 7.91 %	+ 30.36 %	+ 25.18 %
Sig. (2-tailed)	.860	.803	.162	.200

* $\alpha < .05$

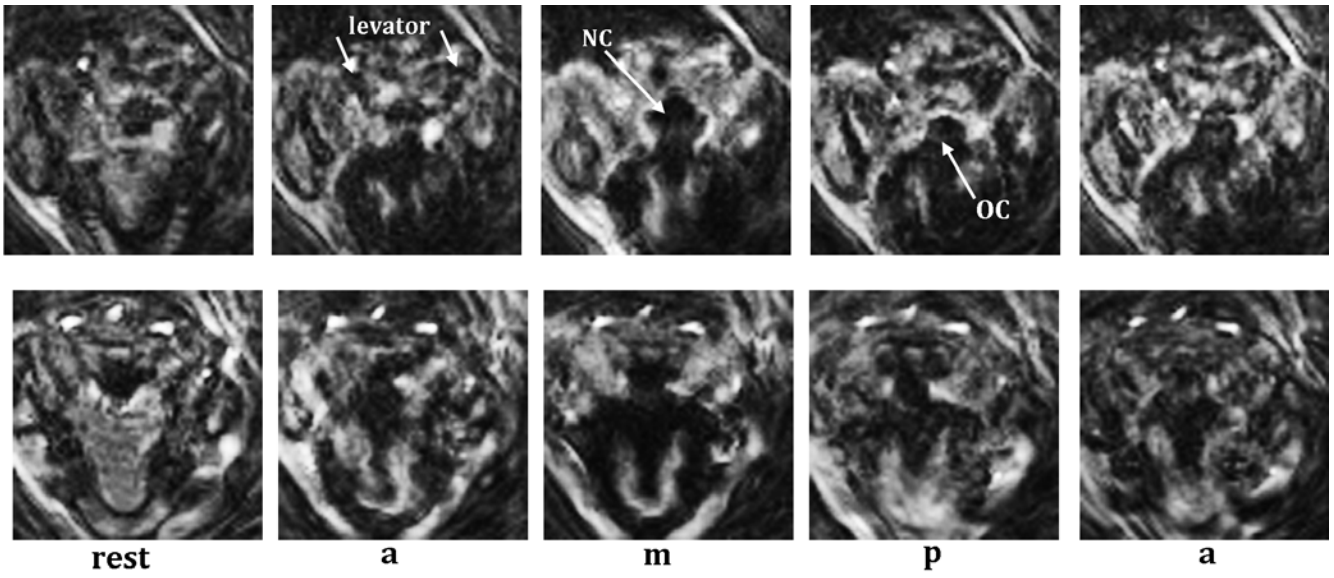

Figure 16. Oblique coronal images of levator muscle at rest and during speech production of "ampa" for one participant with normal anatomy (top row) and one participant with repaired cleft palate (bottom row). NC = nasal cavity; OC = oral cavity; levator = levator veli palatini muscle.

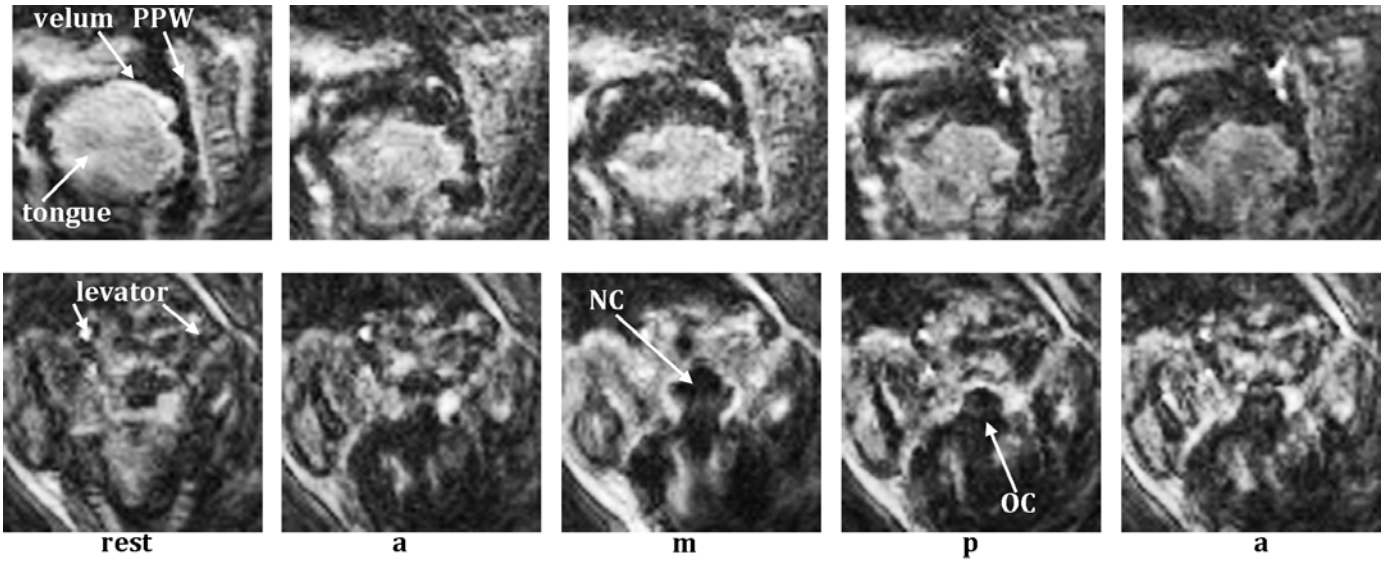

Figure 17. Dynamic midsagittal (top) and oblique coronal (bottom) images of one participant with normal anatomy at rest and during production of phonemes in "ampa." PPW = posterior pharyngeal wall; levator = levator veli palatini muscle; NC = nasal cavity; OC = oral cavity.

Table 16. *Overview of Structural and Functional Differences Observed in Participants with Repaired Cleft Palate Compared to Normal Anatomy*

Structural Differences	
Increased variability?	Yes
Shorter levator muscle?	Not significant
Shorter velum?	Not significant
Shorter hard palate?	Yes
Smaller VP ratio?	Yes

Functional Differences	
Differences in VP function?	Yes
Reduced range of velar motion?	Somewhat
Reduced levator contractility?	Not significant

APPENDIX: IRB APPROVAL LETTER

UNIVERSITY OF ILLINOIS
AT URBANA-CHAMPAIGN

Office of the Vice Chancellor for Research
Institutional Review Board
528 East Green Street
Suite 203
Champaign, IL 61820

April 4, 2013

Brad Sutton
Bioengineering
4157 Beckman Institute
405 N Mathews Ave
MC 251

RE: *MRI of the Velopharyngeal Mechanism*
IRB Protocol Number: 09560

Dear Dr. Sutton:

This letter authorizes the use of human subjects in your continuing project entitled *MRI of the Velopharyngeal Mechanism*. The University of Illinois at Urbana-Champaign Institutional Review Board (IRB) approved the protocol as described in your IRB-1 application, by expedited continuing review. The expiration date for this protocol, UIUC number 09560, is 03/28/2014. The risk designation applied to your project is *no more than minimal risk*. Certification of approval is available upon request.

Copies of the attached date-stamped consent form(s) must be used in obtaining informed consent. If there is a need to revise or alter the consent form(s), please submit the revised form(s) for IRB review, approval, and date stamping prior to use.

Under applicable regulations, no changes to procedures involving human subjects may be made without prior IRB review and approval. The regulations also require that you promptly notify the IRB of any problems involving human subjects, including unanticipated side effects, adverse reactions, and any injuries or complications that arise during the project.

If you have any questions about the IRB process, or if you need assistance at any time, please feel free to contact me or the IRB Office, or visit our Web site at http://www.irb.illinois.edu.

Sincerely,

Anita Balgopal, Director, Institutional Review Board

Attachment(s)

c: John Brockenbrough
Jamie Perry

Telephone (217) 333-2670 • fax (217) 265-5328 • email IRB@illinois.edu